

1-1-2013

## Investigation of Longitudinal Joints Between Precast Prestressed Deck Bulb Tee Girders Using Latex Modified Concrete

Clark Baer  
*University of South Carolina - Columbia*

Follow this and additional works at: <https://scholarcommons.sc.edu/etd>



Part of the [Civil and Environmental Engineering Commons](#)

---

### Recommended Citation

Baer, C.(2013). *Investigation of Longitudinal Joints Between Precast Prestressed Deck Bulb Tee Girders Using Latex Modified Concrete*. (Master's thesis). Retrieved from <https://scholarcommons.sc.edu/etd/2452>

This Open Access Thesis is brought to you by Scholar Commons. It has been accepted for inclusion in Theses and Dissertations by an authorized administrator of Scholar Commons. For more information, please contact [digres@mailbox.sc.edu](mailto:digres@mailbox.sc.edu).

**INVESTIGATION OF LONGITUDINAL JOINTS BETWEEN PRECAST  
PRESTRESSED DECK BULB TEE GIRDERS USING LATEX MODIFIED  
CONCRETE**

by

Clark Baer

Bachelor of Science  
University of South Carolina, 2004

---

Submitted in Partial Fulfillment of the Requirements

For the Degree of Master of Science in

Civil Engineering

College of Engineering and Computing

University of South Carolina

2013

Accepted by:

Paul Ziehl, Director of Thesis

Juan Caicedo, Reader

Fabio Matta, Reader

Lacy Ford, Vice Provost and Dean of Graduate Studies

© Copyright by Clark Baer, 2013  
All Rights Reserved.

## **DEDICATION**

To my wife, whose love, encouragement, and support made this possible.

## **ACKNOWLEDGEMENTS**

First and foremost I would like to thank Dr. Paul Ziehl, who gave me the opportunity to perform this research. I would also like to thank my fellow graduate students and USC staff, including but certainly not limited to: Mohamed ElBatanouny, Marwa Abdelrahman, Matt Jones, Grady Matthews, Michael Miller, Russell Inglett, and Matt Devine. Especially I would like to thank Karen Ammarell for her tremendous help with admissions, administration, and countless other tasks while earning my degree.

Finally, all glory and honor to God, whose grace, mercy, and strength sustained me throughout this endeavor.

## **ABSTRACT**

This study investigates the behavior and performance of latex modified concrete (LMC) as a closure pour material with a U-bar connection detail in longitudinal joints between precast deck bulb tee bridge girders with integral concrete decks. The objective was to determine if the joint detail was capable of resisting service shear and moment stresses as well as eliminate the formation of cracks in the joint during fatigue loading.

This study tested two large scale reinforced concrete slab specimens measuring 6 ft x 6 ft x 8 in joined together by the longitudinal joint detail in fatigue flexure shear loading. The fatigue loading consisted of 2,000,000 cycles at 1.5 Hz and varied between 4.4 and 25 kips. At 500,000 cycle intervals, a service level overload was performed where the specimen was loaded to 46.9 kips. During the fatigue and service level testing, the joint area was inspected visually to determine whether cracks had formed, and a ponding test was initiated after the conclusion of testing to determine whether the joint was water tight.

Vertical through cracking of the longitudinal joint was not detected throughout the study. During the ponding test, water was not seen leaking vertically through the joint, however a slight discharge could be seen at one joint end. Since the leak was in the compressive zone of the joint, it is assumed that this crack developed from drying shrinkage, and not from external loading. Based on the performance of the joint, the U-bar detail with an LMC closure pour is recommended for longitudinal joints in precast deck bulb tee bridge systems.

## TABLE OF CONTENTS

DEDICATION .....	iii
ACKNOWLEDGEMENTS.....	iv
ABSTRACT .....	v
LIST OF TABLES .....	viii
LIST OF FIGURES .....	ix
CHAPTER I: INTRODUCTION .....	1
1.1    BACKGROUND.....	1
1.2    RESEARCH SIGNIFICANCE .....	2
1.3    OBJECTIVES.....	3
1.4    LAYOUT OF THESIS .....	3
CHAPTER II: LITERATURE REVIEW .....	4
2.1    INTRODUCTION.....	4
2.2    HISTORY OF DEVELOPMENT OF REVISED LONGITUDINAL JOINT DETAIL .....	4
CHAPTER III: INVESTIGATION OF LONGITUDINAL JOINTS BETWEEN PRECAST PRESTRESSED DECK BULB TEE GIRDERS USING LATEX MODIFIED CONCRETE.....	31
3.1    EXPERIMENTAL PROCEDURE .....	31
3.2    RESULTS AND DISCUSSION .....	37
3.3    CONCLUSION .....	39
CHAPTER IV: SUMMARY AND CONCLUSIONS .....	59

4.1	SUMMARY .....	59
4.2	CONCLUSIONS .....	60
4.3	RECOMMENDATIONS AND FUTURE WORK.....	60
	REFERENCES .....	62
	APPENDIX A: ADDITIONAL FATIGUE AND SERVICE LEVEL TEST DATA .....	64



## **LIST OF TABLES**

Table 2.1: Results of Closure Pour Evaluation (Li, Et al., 2010) .....	26
Table 3.1: Slab specimen concrete mix proportion .....	40
Table 3.2: Compressive strength of slab concrete .....	40
Table 3.3: Mix designs of closure pour test batches .....	41
Table 3.4: Closure pour concrete properties .....	41
Table 3.5: Residual specimen displacement .....	42

## LIST OF FIGURES

Figure 2.1: Recommended joint details (Li, Ma, Griffey, & Oesterle, 2010) .....	27
Figure 2.2: Finite element model (Li, et al., 2010) .....	28
Figure 2.3: Proposed U-bar connection detail (French, et al., 2011).....	28
Figure 2.4: Large scale specimen dimensions (French, et al., 2011).....	29
Figure 2.5: Large scale specimens prior to pour (French, et al., 2011) .....	29
Figure 2.6: Large scale specimens after pour (French, et al., 2011).....	30
Figure 2.7: Welded plate detail (Gergely, Overcash, Mock, Clark, & Bailey, 2007) .....	30
Figure 3.1: Section view of longitudinal joint detail .....	43
Figure 3.2: Plan view of longitudinal joint detail .....	43
Figure 3.3: Plan view of test specimen .....	44
Figure 3.4: Elevation view of test specimen.....	44
Figure 3.5: Specimen formwork with foam board for shear key .....	45
Figure 3.6: Specimen formwork with tied rebar .....	45
Figure 3.7: View of tied rebar with lift inserts.....	46
Figure 3.8: View of both specimens with rebar .....	46
Figure 3.9: Specimens being moist cured .....	47
Figure 3.10: Specimen after casting and curing.....	47
Figure 3.11: Specimens set in place to form the joint prior to sandblasting.....	48
Figure 3.12: Joint formed with #4 headed bars in position following sandblasting .....	48
Figure 3.13: View of completed joint prior to pour.....	49

Figure 3.14: Joint following closure pour.....	49
Figure 3.15: End view of joint.....	50
Figure 3.16: Burlap and plastic used for curing joint .....	50
Figure 3.17: Shrinkage specimens .....	51
Figure 3.18: Shrinkage test results.....	51
Figure 3.19: View of test set up.....	52
Figure 3.20: Plan view of test set up.....	52
Figure 3.21: Elevation view of test set up.....	53
Figure 3.22: Joint condition following fatigue testing.....	53
Figure 3.23: Underside of joint after fatigue loading .....	54
Figure 3.24: View of ponding test .....	54
Figure 3.25: Leaking at end of joint.....	55
Figure 3.26: Fatigue cycle F1 deflection over time .....	55
Figure 3.27: Fatigue cycle F2 deflection over time .....	56
Figure 3.28: Fatigue cycle F3 deflection over time .....	56
Figure 3.29: Fatigue cycle F4 deflection over time .....	57
Figure 3.30: Load vs. deflection for fatigue cycle F3.....	57
Figure 3.31: Load vs. deflection for service level overload 1 .....	58
Figure A.1: F1 load versus time.....	64
Figure A.2: F1 Load versus deflection .....	65
Figure A.3: F2 Load versus time .....	65
Figure A.4: F2 Load versus deflection .....	66
Figure A.5: F3 Load versus time .....	66

Figure A.6: F4 Load versus time .....	67
Figure A.7: F4 Load versus deflection .....	67
Figure A.8: Load vs. deflection for service level overload 2.....	68
Figure A.9: Load vs. deflection for service level overload 3.....	68

# **CHAPTER I**

## **INTRODUCTION**

### **1.1 BACKGROUND**

In an effort to further reduce costs and traffic disruption, rapid bridge construction techniques are being actively developed and investigated to determine the reliability and safety of the structures produced using these methods. Current practice limits this type of construction to lightly traveled short span bridges using prestressed hollow core sections. However, in some areas of the US such as the Pacific Northwest, longer span bridges are being built from prestressed deck bulb tee girders with reinforced decks cast integrally with the girder. As with hollow core sections, this eliminates the need for a cast in place deck over the girders. This method brings the benefits of rapid construction to roads which see heavier traffic and require longer spans.

Current use of this type of construction has demonstrated the adequacy of the longitudinal joints to resist the dead and live loading. Durability, however, has proven to be a concern. Over the service life of the bridge, excessive cracking of the longitudinal joint has been encountered, leading to moisture and chloride penetration of the joint, resulting in corrosion of the reinforcing steel and increasing the risk of premature failure. Recent research has been undertaken to develop new longitudinal connection details as well as new closure pour materials in an effort to correct this deficiency.

The most common detail currently in use consists of a shear key with an embedded steel angle, to which a steel plate is welded at 5 foot centers along the length

of the bridge. This detail adequately resists vertical and longitudinal shear, but exhibits poor moment resistance. The National Cooperative Highway Research Program project 10-71 titled “Cast-in-Place Concrete Connections for Precast Deck Systems” (French, et al., 2011) resulted in the development of a revised detail, consisting of #5 U-bar reinforcing embedded in the deck protruding transversely into the joint with #4 headed lacer bars threaded through the linked U-bars. This detail, used with a high performance concrete closure pour material, demonstrated improved moment resistance; however small cracks formed in the tensile zone of the joint under service loading.

The cracks which developed were primarily at the interface between the cast in place closure pour and the precast deck. In order to reduce interface cracking, a closure pour material would need to have high bond strength with pre-existing concrete. There are several products on the market which have this property, however a material that is already in widespread use would have the advantages of reduced cost and familiarity on the part of contractors and design professionals. Latex modified concrete was used as the closure pour material for this study, as it possesses higher bond strength than standard concrete, and is already used frequently as a bridge deck overlay.

## **1.2 RESEARCH SIGNIFICANCE**

In the program described herein, representative slab specimens were joined using latex modified concrete (LMC) for the closure pour material and then tested in flexure-shear at the University of South Carolina Structures Laboratory. The joint demonstrated improved crack resistance at service level and fatigue loading and remained water tight following the testing regimen. Small amounts of water seepage were encountered due to cracks

forming from drying shrinkage. These results recommend LMC as a closure pour material for longitudinal joints in precast bridge systems.

### **1.3 OBJECTIVES**

The primary objective of this study was to determine the performance of LMC as a closure pour material using the revised longitudinal connection detail. It was proposed that the improved bond and tensile strength of LMC would reduce or eliminate cracking at service level loads. The specific objectives can be summarized as follows:

1. Design and construct representative slab specimens conforming to the 2006 SCDOT Bridge Design Manual (SCDOT, 2006)
2. Design LMC mix for use as closure pour material
3. Subject specimens to a fatigue testing program and compare performance of joint with results from NCHRP 10-71

### **1.4 LAYOUT OF THESIS**

The Thesis consists of four chapters. In Chapter II, a literature review is presented that describes the commonly used and recently developed longitudinal joint details in precast deck bulb tee bridges. A summary of some of the studies which are relevant to this case study are presented.

Chapter III is titled “Investigation of the Behavior of Latex Modified Concrete as a Closure Pour Material in Longitudinal Joints between Precast Slabs”, where the experimental study conducted in the USC Structures Lab is presented.

Chapter IV includes a summary of the Thesis as well as conclusions based on this study. Recommendations for further research are also provided in this chapter.

## **CHAPTER II**

### **LITERATURE REVIEW**

#### **2.1 INTRODUCTION**

Numerous studies have been conducted in the previous decade on the construction of bridges using precast prestressed deck bulb tee girders. These investigations were performed to better understand the behavior of bridges built using this construction method, and how to improve durability of the longitudinal joint. These studies culminate in the revised longitudinal joint detail, however cracking had not yet been fully eliminated at service level loading. An overview of the work that was performed in developing the revised detail as well as studies of prototype bridges is presented in this chapter.

#### **2.2 HISTORY OF DEVELOPMENT OF REVISED LONGITUDINAL JOINT DETAIL**

**Li, Ma, Griffey, and Oesterle (2010), “Improved Longitudinal Joint Details in Decked Bulb Tees for Accelerated Bridge Construction: Concept Development”**

Li, Ma, Griffey, and Oesterle [2010] conducted this study to investigate improved continuous longitudinal joint details for decked precast concrete girder bridge systems. Multiple candidate details were developed, and were then subjected to discussion by design engineers and bridge construction contractors, as well as municipal departments of transportation. Following this stage, a reduced list of details was investigated further.



The proposed new connection details were designed to better control cracking, while maintaining rapid constructability. The suggested details were as follows:

- Hooked bars (U-bar)
- Headed bars
- Bars confined by spiral reinforcement

A survey of bridge professionals was conducted to gauge the potential constructability and structural viability of each detail. The results indicated that the spiral reinforcement detail was universally considered to have low constructability, while U bars and headed bars were seen as superior with the headed bar detail given the most favorable response. Thus, the experimental program was conducted using this detail as well as interlocking welded wire reinforcement for comparison.

Each model specimen was 2 feet wide, 10 feet long, and 6 inches deep. Three types of specimens were tested: lapped headed bar, WWR, and a control specimen with continuous reinforcement throughout the span. The tested variables for the headed bars were lap length and the spacing of the reinforcement, while for the WWR the only variable was spacing. Lap lengths of 2.5, 4, and 6 inches were used. The control specimen was reinforced with continuous #5 bars spaced 6 inches. The headed bar connection consisted of staggered, lapped #5 bars, with one longitudinal #5 bar laid in the center of the lap of the transverse bars. The eight total specimens were cast monolithically with a 28-day design concrete strength of 7,000 psi. Cylinders were taken to determine the actual  $f'_c$  on the testing day. Strain gauges were placed in the joint zone to better describe the behavior of the details under load. Specimens were simply supported and loaded with two equal loads spaced at 40 inches about the center of the

span with the joint zone experiencing constant moment and no shear. The measured parameters were deflection, curvature, and settlement.

Specimens using WWR and headed bar with lap lengths less than 6 inches exhibited brittle failure, and were therefore deemed unacceptable. Specimens with headed bar reinforcement lapped 6 inches and the control specimen exhibited ductile behavior under load, indicating the reinforcement steel was yielding once the nominal moment was reached, and that the specimens had adequate anchorage capacity to fully develop the reinforcement. The 6 inch lap specimens also exhibited greater cracking control, indicated by a 0.004 inch crack developing under assumed service load conditions. Moment capacity for the 6 inch lap specimens were 39.4 ft-kips and 25.83 ft-kips for the 4 inch spacing and 6 inch spacing, respectively.

Based on the results of the survey and experimental program, a 6 inch lapped headed bar detail is recommended to replace the current welded steel connector. This recommendation is based on moment capacity, curvature, cracking control, deflection, and steel strain comparison.

**Li, Ma, and Oesterle (2010), “Improved Longitudinal Joint Details in Decked Bulb Tees for Accelerated Bridge Construction: Fatigue Evaluation”**

Li, Ma, and Oesterle [2010] conducted this study to investigate the response of the lapped headed bar detail to fatigue loading when used in longitudinal joints between decked bulb tee bridge girders. Four full scale slabs were fabricated using #5 headed bars lapped 6 inches for the longitudinal connection. An analytical parametric study was formulated based on these specimens to determine the maximum forces generated in the longitudinal joint when the slab is subjected to service loads. Subsequently, the slabs were loaded both

statically and cyclically using four-point flexural and three-point flexural-shear loading. Results were compared between the static and fatigue testing based on flexural capacity, curvature, cracking, deflection, and strain in the reinforcing steel.

The parametric study consisted of finite-element models of seven bridge configurations that varied by girder depth, girder spacing, span, and bridge skew. The range of girder depth was 41 to 65 inches, the range of girder spacing was 4 to 8 feet, the spans ranged from 82 feet 8 inches to 132 feet, while the bridge width was constant at 40 feet. The models were loaded based on the AASHTO LRFD Bridge Design Specification's live load HL-93, which consists of a design vehicle load and lane load. This loading was adjusted to provide the greatest possible force in the longitudinal joint. The parametric study indicated the following findings:

- The maximum forces in the joint were not sensitive to the length of the lane load
- In the longitudinal direction, the impact of the location of the vehicle load on the maximum forces in the joint was not significant
- The maximum forces in the joints were not sensitive to the span of the bridge
- Larger moment and shear forces were produced in DBT girders with larger spacing and shallower depth
- Single lane loading produced larger forces than multilane loading and it dominated the loading level
- The maximum positive moment, negative moment, and shear were 7.922 kips ft/ft, -2.152 kips ft/ft, and 6.091 kips/ft, respectively, before cracking.
- After cracking, the maximum positive moment, negative moment, and shear were 4.001 kips ft/ft, -1.137 kips ft/ft, and 5.056 kips/ft, respectively.

- Under fatigue live loading the maximum positive moment, negative moment, and shear were 2.143 kips ft/ft, -0.453 kips ft/ft, and 2.326 kips/ft, respectively.

In the experimental program, four slabs measuring 72 inches wide, 64 inches long, and 6 inches deep were fabricated for the static and fatigue testing. A female to female shear key was provided on both lateral edges to allow each slab to be used for two tests. The slabs were reinforced with five layers of reinforcement, with the headed bars coated with epoxy and projecting out of the slab into the shear keys, as illustrated in figure 5. The design 28-day compressive strength of the concrete was 4,000 psi.

Following fabrication of the slabs, the shear keys were sandblasted prior to constructing the joint. SET 45 HW grout was poured into the gap between the slabs around the headed bars to form the connection in accordance with the improved longitudinal joint detail. The slab specimens were tested under four different conditions: flexure static, flexure-shear static, flexure fatigue, and flexure-shear fatigue. Linear voltage displacement transducers and strain gauges were installed to measure the deflection, settlement, curvature, and strain. Flexure-only specimens were loaded with two symmetric loads equidistant from the longitudinal joint, while flexure-shear specimens were loaded with one load located 12 inches from the joint.

The fatigue loadings were developed from the results of the parametric study. First, a static loading was applied in increments up to 22.7 kips in order to produce the maximum positive moment of 7.922 kips ft/ft and to crack the joint. The specimen was then subjected to a negative moment of -2.152 kips ft/ft and unloaded to zero. Next, a fatigue loading cycle was initiated, where alternating moments of 2.143 kips ft/ft and -0.453 kips ft/ft were applied for a total of 2 million cycles at a frequency of 4 Hz.

Intermittent with the fatigue loading, static loading was applied after completion of 0.5, 1.0, 1.5, and 2.0 million cycles. Following the fatigue loading the specimen was statically loaded until failure.

Comparison of the fatigue-loaded girders with the statically loaded girders indicated little to no difference in curvature, strain, and overall load capacity. However, fatigue did inhibit the development of a plastic hinge in the girder after the reinforcement yielded, leading to a significant reduction in ductility. While increased safety factors and other precautions should be taken due to the increased probability of brittle failure that would be caused by lessening of ductility, on the whole these results recommend the improved headed bar longitudinal joint detail as viable for precast decked bulb tee bridge girders.

#### **Zhu and Ma (2010), “Selection of Durable Closure Pour Materials for Accelerated Bridge Construction”**

Zhu and Ma [2010] conducted this study to develop reliable criteria for selection of closure pour material for joining precast bridge girders used in accelerated bridge construction. A wide variety of materials are currently available, each with unique advantages and disadvantages depending on construction type, environmental setting, and load requirements. This study divides the candidate materials into two categories: overnight cure and 7-day cure. A literature review was conducted to assemble a list of commonly used products and establish preliminary criteria, followed by testing for compressive strength and workability to reduce the list to 2 candidates in each category. Final performance criteria are then developed based on durability tests of the selected

candidate materials. Durability tests include freezing-and-thawing, shrinkage, bond, and permeability.

An extensive literature review was first conducted to develop preliminary performance criteria. The materials were divided into three grades, each with differing requirements. Based on the headed bar detail recommended by Li et al. (2009), it was found that the minimum compressive strength necessary to develop the headed bars would be 6.0 ksi. For cracking, the Colorado Department of Transportation Specifications Committee (2005) specified that Class H concrete used for bare concrete bridge decks must not exhibit a crack at or before 14 days in the cracking tendency test (AASHTO PP 34-39). For chloride penetration, a percent chloride of 0.2% by mass of concrete must not be present beyond 38mm deep after 90 day ponding. The criterion for bond strength was developed based on the Li et al. (2009) parametric study that suggested the maximum shear stress in longitudinal joints due to live loads is 84 psi. Therefore, a minimum limit of 200 psi was proposed. For freezing and thawing durability, the relative dynamic modulus of elasticity must be greater than 70%, 80%, and 90% in Grades 1, 2, and 3 respectively after 300 cycles. This result was based on Russell and Ozyildirim (2006). Additionally, mixes containing aggregates must prevent alkali-silica reactivity and delayed ettringite formation. The former can be accomplished by establishing an upper limit on 14-day expansion at 0.10%, and Folliard et al. (2006) suggested requiring that internal concrete temperatures not exceed 158°F to prevent the latter.

Published performance data for the different materials were used in assembling a preliminary list. The overnight cure grouts were then tested for compressive strength and workability, with EUCO-SPEED MP and Set 45 HW performing better than the other

options. 7-day cure grouts were tested for compressive strength at 7 days, shrinkage, chloride penetration, and freezing-and-thawing durability. HPC Mix 1 and RSLP Mix 2 were selected based on their superior responses to the four criteria.

The four selected materials were then subjected to long term tests, including: freezing-and-thawing durability (ASTM C666 Procedure A modified), shrinkage (AASHTO Designation: PP34-39 modified), bond (ASTM C882 modified), and permeability (ASTM C1543 modified). Based on the observed responses, the values found in Table 2.1 are recommended.

As indicated by the literature review and long term testing, grout or concrete meeting the specified values in Table 2.1 would adequately perform as closure pour material in longitudinal joints between precast bridge girders.

#### **Ma, Chaudhury, Millam, and Hulsey (2007), “Field Test and 3D FE Modeling of Decked Bulb-Tee Bridges”**

Ma, Chaudhury, Millam, and Hulsey [2007] conducted this study to determine the effect of shear connectors and intermediate diaphragms on live-load distribution and connector forces in decked, precast, prestressed, bulb tee bridge girders. A 3D finite element model was developed and then calibrated using bridge load testing results from an ongoing research project at the University of Alaska Fairbanks. Subsequently, a parametric study investigating the live load distribution response to varying configurations of shear connections and intermediate diaphragms was conducted using the calibrated FEM.

The field testing program was comprised of eight separate bridges subjected to continuous and static loads at defined transverse locations. Each bridge was equipped with strain gauges to measure shear and flexural strain. Strains measured from continuous

loading were used to identify maximum strain and maximum live load distribution factors (DFs), while strains measured from static loading were used to calibrate the FEM.

The finite element model treated the bridge as a 3D system, using 20-node brick elements for the deck and girders, 2-node hinge-connector elements for shear connectors, and 3D truss elements for the intermediate steel diaphragms. Boundary conditions for the FEM are as follows:

- One end of the bridge is assumed to be roller supported and restrained in the vertical and transverse directions, while free in the longitudinal direction
- The other end of the bridge is assumed as pin connected and restrained in the vertical, transverse, and longitudinal directions

Comparison of the FEM with the experimental results showed general agreement and that the FEM could be reliably used for the parametric study.

The parametric study calculated strains in the diaphragms and longitudinal shear connectors based on the following configurations:

- Five intermediate steel diaphragms uniformly distributed along the span
- One diaphragm located at midspan only
- No diaphragm in the bridge
- 28 shear connectors evenly spaced
- 14 shear connectors evenly spaced
- 7 shear connectors evenly spaced

Once strains were calculated, the distribution factor for moment was then determined using the following equation:

$$DF_{moment} = \frac{\varepsilon_x}{\varepsilon_1 + \varepsilon_2 + \varepsilon_3 + \varepsilon_4 + \varepsilon_5}$$



DFs for different connection, diaphragm, and loading configurations were compared, as well as forces in the longitudinal connectors.

It was found that the live load DF for a single-lane loaded bridge was smaller than for a double-lane loaded bridge. This suggests that revision of the relevant articles in the AASHTO LRFD Specifications, which use one equation for each scenario, should be considered. Also, DFs for bridges without diaphragms is higher than those with diaphragms, however the total number of diaphragms has little influence. For the shear connectors, increasing connector spacing causes the maximum horizontal shear force to increase, while having little effect on vertical and in-plane normal tensile forces. Conversely, connectors next to the wheel loads tend to have a higher vertical shear force and a higher in-plane normal force. Lastly, summation of the connector forces in each direction along the longitudinal joint produces a constant value regardless of the number of connectors in the joint.

**Oesterle, Elremaily (2009), “Design and Construction Guidelines for Long-Span Decked Precast, Prestressed Concrete Girder Bridges”**

Oesterle, Elremaily [2009] conducted this study to establish recommended design and construction specifications for long-span decked, precast, prestressed concrete girder bridges. This report incorporates the results from the investigations outlined in the previous four studies in this review, as well as gives suggested design and construction guidelines based on those results. The objectives for this study are to address common concerns with this type of construction, provide guidance to those inexperienced with DPPCG, and update the relevant portions of the AASHTO LRFD Bridge Design Specifications.

Despite the advantages of using DPPCG, their widespread use has long been confined to the Pacific Northwest, where this type of bridge has been used very successfully. This is largely due to perceived problems with their structural integrity, such as connections between adjacent units, longitudinal joints, longitudinal camber and cross slope, live load distribution, continuity for live load, lateral load resistance, skew effects, maintenance, and replaceability. To address these issues, the report first documented the successful methodologies in use today, determined the most efficient girder section, suggested possible methods of deck replacement, and developed and tested improved longitudinal connections.

Since DPPCG bridges have been used successfully for some time, the study focused on the remaining areas of concern barring more widespread use. In an effort to reduce girder weight to facilitate easier transportation from fabrication site to the project, a parametric study was conducted to determine the most structurally efficient section. Girder depths of 41 in, 53 in, or 65 in were considered with four different bottom bulb geometries tested for each depth. Normal, tall, wide and NU configurations were tested. A 6 in top flange thickness, 8-ft flange width, and 6 in web thickness were assumed. The NU bulb configuration was shown to be the most efficient in all cases.

Most current applications for DPPCG bridges are in low-traffic scenarios, which as a result are not designed to facilitate deck replacement as part of the maintenance program. Typically, the high performance concrete used in DPPCGs outlasts the design life of the bridge. This, combined with the ease and rapidity of construction, make it more economical in some cases to replace the entire superstructure of the bridge as opposed to the deck only. For higher traffic situations, the study researched design strategies to allow

for efficient deck replacement in DPPCG bridges. NCHRP Report 407 suggested the use of a shear key system with a debonded interface between the precast girder and the cast-in-place deck. It was recommended that this interface be used between the subflange and flange in DPPCGs that are cast in two phases to allow for ease of deck removal and replacement.

The primary concern given by industry experts as part of the initial survey conducted in the study is the durability and performance of the longitudinal joint. To address this, analytical studies were carried out to determine the maximum forces in the joint as a result of differential camber and live load forces. The analytically obtained values were then used to experimentally test candidates for improved headed bar details, as outlined in Li et al (2010) and Li et al (2011). The headed bar detail was shown to have sufficient strength, fatigue characteristics, and crack control for the maximum loads determined from the analytical studies and is a viable connection system for DPPCGs.

Based on the literature review, analytical results, and experimental results, suggested comprehensive design guidelines were laid out for adoption by AASHTO and use by groups interested in constructing a prototype bridge for evaluation and testing. The guidelines include the improved longitudinal detail, recommended deck replacement design, and the optimized family of girder sections.

**French, Shield, Klaseus, Smith, Eriksson, Ma, Zhu, Lewis, and Chapman (2011),  
“Cast-in-Place Concrete Connections for Precast Deck Systems”**

French, Shield, Klaseus, Smith, Eriksson, Ma, Zhu, Lewis, and Chapman [2011] conducted this study to determine recommended design and construction specifications for cast in place reinforced concrete connections for precast deck systems. This report

combines previous work done at the University of Tennessee – Knoxville (cited above), as well as work done by researchers at the University of Minnesota – Twin Cities on precast composite slab span systems. This review will focus on the results presented for the decked bulb tee sections.

Possible connection concepts for joining the precast DBT girders were weighed using a phone survey of industry professionals. The choices were then narrowed down based on performance, cost, and ease of construction. The three connection details found to be superior were lapped headed bar reinforcement, lapped U-bar reinforcement fabricated with deformed wire, and lapped U-bar reinforcement fabricated with stainless steel. Each detail was tested in both flexure and tension to simulate conditions encountered in longitudinal and transverse joints, respectively. The two U-bar details were found to have higher capacity and smaller crack widths at service level loading. In previous studies, the U-bar detail encountered resistance due to the required bend radius being smaller than the ASTM standard due to thin bridge decks. The use of deformed wire or highly ductile stainless steel alleviated this concern; however the high cost of the stainless steel led to the selection of the deformed wire as the most cost efficient choice. Constructability of the U-bar deformed wire detail was also found to be superior to the headed bar detail, as it created a less congested joint. Upon consideration of all these factors, the U-bar deformed wire detail was selected for further testing, including an additional round of six specimens tested for flexure and tension. Based on the results, the authors recommended the joint overlap length should not be less than 6 inches and #4 lacer bars should be provided along the joint to enhance mechanical anchorage, provide adequate ductility, and prevent significant loss of strength at ultimate load.

Following selection of the U-bar detail, a parametric study was conducted to create a database of maximum forces in the longitudinal joints to determine the forces to be used in the large scale static and fatigue testing. Two sections were tested, a decked bulb-T girder (DBT65) and a bulb-T girder (BT72). First, a 3D FE model of the bridge was developed using ABAQUS, then a HL-93 live load was applied, and the effects of loading location, bridge width, truck/lane loading versus tandem/lane loading, girder geometry, bridge skew, single-lane versus multi-lane, and cracking of the joints were evaluated. The controlling load cases were determined by positioning the transverse joint over an interior support. It was conservatively assumed that the bridge deck would resist the tension force created by the resulting negative moment. The following forces were found:

- Maximum moments in transverse joints were -3140 kip-ft/beam design, -910 kip-ft/beam fatigue, 503 kip-ft/beam design, and 196 kip-ft/beam fatigue for DBT65, the controlling case
- Transverse stresses of the U-bar in girder DBT65 were 35.6 ksi and 10.3 ksi under negative design load (-3140 kip-ft) and negative fatigue load (-910 kip-ft) respectively, based on cracked section analysis

Performance criteria were then developed for durable closure pour materials for the longitudinal and transverse joints. Overnight and 7-day cure materials were tested for freezing-and-thawing durability, shrinkage, bond, and permeability tests, with the final criteria being as presented in Table 2.1.

Specimens were then fabricated for a full scale fatigue and static load testing program as outlined in Li (2010) above.

It was found that fatigue loading had little influence on the behavior of the longitudinal joints, with the exception of specimens using the overnight cure closure pour material. After 2 million cycles, overnight cure specimens had less load capacity than similar specimens subjected to static loading only. For the transverse joints, excessive crack widths were found when using 75 ksi steel as opposed to 60 ksi steel. It is recommended that 60 ksi steel and larger bars be used if stresses in the reinforcement are not limited at service. Overall, the U-bar detail performed well throughout the fatigue and static loading program.

Comprehensive design and construction specification recommendations for decked bulb tee girder longitudinal connections were presented as a result of the study. Revisions to the AASHTO LRFD Specifications on topics including minimum bar bend, minimum depth and cover, precast deck slabs on girders with longitudinal and transverse joints, and decked bulb tee decks were suggested as well. Five example design problems were formulated to demonstrate application of the results. This report revised the recommendation of earlier studies on the topic, as it recommended the U-bar detail with deformed wire over the headed bar detail.

**Gergely, Overcash, Mock, Clark, and Bailey (2007), “Evaluation of Design and Construction of HPC Deck Girder Bridge in Stanly County, North Carolina”**

Gergely, Overcash, Mock, Clark, and Bailey [2007] conducted this study to investigate the behavior of a highway bridge built with high performance, precast, prestressed, decked bulb-tee girders. The study consisted of a preliminary design submitted by the NCDOT which was compared to a parametric study performed using Larsa™ 2000 4<sup>th</sup> Dimension for Bridges (Larsa™, 2005). An ANSYS™ finite element model of the bridge

was then developed to analyze the behavior of the steel plates and steel diaphragms connecting the girders as well as the stresses throughout the structure. The values produced by the FE model were then compared to laboratory testing of the welded steel plate connectors. Finally, the girders were fabricated and the bridge was installed on site, where it was subjected to static and dynamic load testing.

The bridge was designed to be two lane, with a bearing to bearing span of 106' with no intermediate supports and with integral end bents. The structure consists of five 107'-4" independent prestressed deck girders connected with welded steel plates at 5'-0" on center and steel diaphragms located at quarter and half points. The girder was fabricated in two phases, first a standard Type III AASHTO girder was cast, then the 6'6" deck section was cast using the same concrete mix as the girder. Once installed on site, the diaphragms and welded steel plates were installed, and the shear key was filled with non-shrink grout.

Following submission of the preliminary design, a parametric study using Larsa™ was conducted. The bridge was assumed to be simply supported, and the software necessitated treating the longitudinal plate connections as welded on the four corners, instead of the fillet weld that was actually used. These factors resulted in a more flexible and weaker connection, causing the analytical study to predict higher forces in the connecting plates. As a result, this initial study was viewed as qualitative in nature, and was used to determine the location of instrumentation on the final bridge. Comparison between the NCDOT design calculations and the Larsa™ model indicated highly consistent results, validating the reliability of the model for further analysis. Stresses were then obtained based on the LRFD Strength I – Truck 3 Loading combination based

on a design with and without diaphragms, which demonstrated that the absence of diaphragms produced stresses in the connection plates well beyond the estimated pull-out capacities. It also showed that the highest stresses in the diaphragms represented only 18% of the material's yield stress.

A construction economy analysis was conducted by comparing costs of building three different bridges of similar span but dissimilar designs. The decked bulb-tee bridge was found to have the highest net cost, most likely due to the girder section being a new design, with no previous examples in existence. It is likely that as these types of girders become more commonly used, the prices will decrease over time.

For further analysis, a FE model was developed using ANSYS™ and calibrated with the LARSA™ model, the provided NCDOT calculations, and the results of the experimental load testing. This model was used to test the effects of plate spacing on the stresses produced in the diaphragms and plate connections, to determine the distribution factor due to live loading, and find the stress field throughout the structure. The highest normal stresses in the top fibers were found to be 902 psi and 712 psi in tension and compression, respectively.

The welded plate flange connections were experimentally tested in tension and longitudinal shear to determine their capacity for load transfer between girders. The average failure loads in tension and shear were 12,778 lbs and 24,646 lbs, respectively. Comparison of experimental results with calculations using the PCI design handbook revealed inconsistent results underscoring the unpredictability of this particular connection. It was recommended that when employing connection details not found in current guidelines, the details should be evaluated using experimental investigation.



Following design, the girders were fabricated and transported on a convoy of five trucks from Savannah, GA to the project site. For transportation, a six axle truck was used, and an extended load permit was obtained. Four lane or larger highways were predominantly traveled and two escorts were provided to each truck. Following construction, a 4" layer of asphalt was added due to the bridge's location at the bottom of a sag curve. It was recommended that when asphalt is not needed, an extra inch of concrete should be added to the top of the deck that can be ground down to provide a smoother riding surface and adjust for elevation after the girders are installed.

Once completed, the bridge underwent load testing prior to opening. Monitoring was accomplished with three instruments: displacement transducers, strain transducers, and strain gauges, all of which were connected to the Data Acquisition System (DAQ). Quasi-static and dynamic loading by two tandem trucks weighing 100,000 lbs total was provided based on a SAP2000™ model to achieve a moment that was approximately 70% of the design moment of 1,632 k-ft. Five different load paths were used to reach maximum stress in each girder. Results of the load testing was as expected, stresses in the members were dependent on load location, and were not uniformly distributed. The FE data and experimental data compared favorably, and indicate the reliability of ANSYS™ and Larsa™ as analysis tools for these types of bridges.

Overall fabrication and construction of the bridge presented no major problems and was completed as designed. Possible improvements include additional tie down locations for transport, 1-inch additional deck height if asphalt will not be applied for a smooth surface, use of lightweight concrete, and development of formwork to allow for one-pour fabrication. Mechanical behavior of the bridge was found to be consistent with

analytical and design results, with the exception of the welded plate longitudinal connection, which will require revised design equations or the use of modeling for future projects. This decked girder type was demonstrated as a viable alternative in rapid bridge construction, and should become more economical as widespread use occurs.

**Holland, Dunbeck, Lee, Kahn, and Kurtis (2011), “Evaluation of a Highway Bridge Constructed Using High Strength Lightweight Concrete Bridge Girders”**

Holland, Dunbeck, Lee, Kahn, and Kurtis [2011] conducted this study to investigate the behavior of a highway bridge constructed from high strength lightweight concrete (HSLW) instead of high strength normal weight concrete. Increasing concrete strength has allowed progressively longer bridge spans to the point where the limiting factor is the capacity of current infrastructure to tolerate loads imposed by transportation of the girders to the project site. Development of new lightweight concrete mixtures is a possible solution to this difficulty; however verification of the reliability of current design practices to accurately predict behavior of the resulting composite structure is necessary prior to broad implementation.

This study presents the findings of an ongoing performance evaluation of the I-85 Ramp “B” Bridge crossing SR-34 in Coweta County, Georgia. The girders are AASHTO BT-54 cross-sections with a 107 foot 11 ½ inch length cast with a 10,000 psi design strength HSLW mix with a unit weight of 120 lb/ft<sup>3</sup>. The deck was constructed with 3,500 PSI normal weight concrete. Vibrating wire strain gauges, taut wire system, thermocouples and a total station were employed to measure prestressing losses, camber, coefficients of thermal expansion, creep, shrinkage, elastic modulus, and stiffness. These

experimentally derived parameters were compared against a variety of standard predictive methods to determine their validity when HSLW is used.

To determine the actual compressive strength of the light weight concrete, over 240 cylinders were tested at 7, 28, 56, and 180 day intervals. The 56 day compressive strength of 10,240 psi was compared against the value obtained by Meyer (2002) for the same mix design and was found to be 11.3% lower. It was concluded that this was due to the lightweight aggregate not being fully saturated prior to construction. All girders met the prescribed design strength by 56 days of age.

While able to exhibit high strength, HSLW possesses a significantly lower modulus of elasticity than normal weight concrete. Elastic moduli were experimentally measured in accordance with ASTM C 469 and were compared with the methods suggested by Lopez (2005), AASHTO LRFD (2007), ACI 363 (1997), Meyer (2002), Cook and Meyer (2006), and the National Cooperative Highway Research Program (2007). Additionally, a load test was performed at 56 days of age on each bridge girder and deflection was measured using a taut wire system, resulting in a calculated modulus of elasticity. The apparent elastic modulus in the girders was computed as 4,190 ksi, which is 12.5% larger than that determined from cylinder testing according to ASTM C 469, the data from which was widely scattered. The equations suggested by Meyer (2002) were determined to most closely match the experimental data from load testing, providing an estimate within 3%. All other methods under-predicted the modulus, except AASHTO which overestimated by 6%.

Coefficient of thermal expansion tests were conducted in accordance with CRD-C 39 (1981). The measured values were lower than normal weight concrete, and were used to adjust the raw data for determination of internal strains throughout the project.

Creep and shrinkage studies were conducted according to ASTM C 512 (2002) and compared with various prediction methods including AASTHO LRFD (2007), ACI 209 (1992), and Lopez (2005). The HSLW was found to have much lower observed creep than estimated by the AASHTO and ACI, while higher than estimated by Lopez, with approximately 90% of the observed shrinkage losses occurring in the first 110 days. Shrinkage and creep data show that after 200 days of age, no significant increases in strain occurred in the HSLW.

A load test and finite element model were employed to characterize the composite behavior of the bridge system and to compare observed behavior with analytical predictors. The bridge was divided into quarter-span (LT1), mid-span (LT2), and three-quarter-span (LT3) partitions. For the FEM, the contribution of prestressed bars and steel reinforcements to the behavior of the bridge were neglected, as the loading did not induce cracking in the concrete. Also, concrete material properties were assumed to be linear elastic, with the modulus of elasticity of the deck and girder calculated to be 3,995 ksi and 4,096 ksi respectively. The measured deformations differed from the predicted values by a maximum of 0.09 inches, 0.07 inches, and 0.04 inches in LT1, LT2, and LT3, respectively. The predicted values were larger with the exception of girders 1 and 2 in LT3. These data indicate that the as-built structure was stiffer than that predicted by the FEM, possibly due to variations in the deck properties. Overall, FEA proved to be a viable analytical technique in modeling HSLW.

878 days of experimental data were collected from the VWSG's to compute prestress loss. Regression analysis allowed extrapolation to 40 years, and indicated a total loss in that time period of 56.1 ksi. These results were compared with six common methods of prestress loss prediction: PCI Design Handbook (2004), ACI 209 (1992), AASHTO LRFD (2007) lump sum and refined, Tadros (Tadros, et al., 2003), and Lopez (2007). All methods with the exception of the PCI Design Handbook were within 4% of the measured loss. The AASHTO LRFD Refined method over-estimated losses by 5%, and provided the best estimate of total losses from all sources, including creep and shrinkage.

The Washington State Department of Transportation (Rosa et. Al., 2007) and PCI Design Handbook (2004) methods of predicting camber induced by prestressing were compared against measured values. Both methods over-predicted the observed value, with the WSDOT method having a difference of 0.08 inches and the PCI method differing by 2 inches.

The performance of the HSLW concrete in this bridge demonstrates its ability to allow for long spans while decreasing weight and allowing for more flexibility in fabrication and delivery. Further, comparison of standard design and analysis techniques with experimental observation of the behavior of the composite structure confirmed the validity of those techniques in HSLW bridge design. These results recommend use of HSLW in future infrastructure projects as a possible time and cost saving strategy.

Table 2.1: Results of closure pour evaluation (Li, Et al., 2010)

Compressive Strength	41.4 MPa At 8 hours (for overnight cure) At 7 days (for 7-day cure)
Shrinkage	No cracks found before 20 days of age
Bond strength	2.5 MPa
Chloride Penetration	Depth of percent chloride of 0.2% by mass of cement after 90 day ponding less than 38 mm

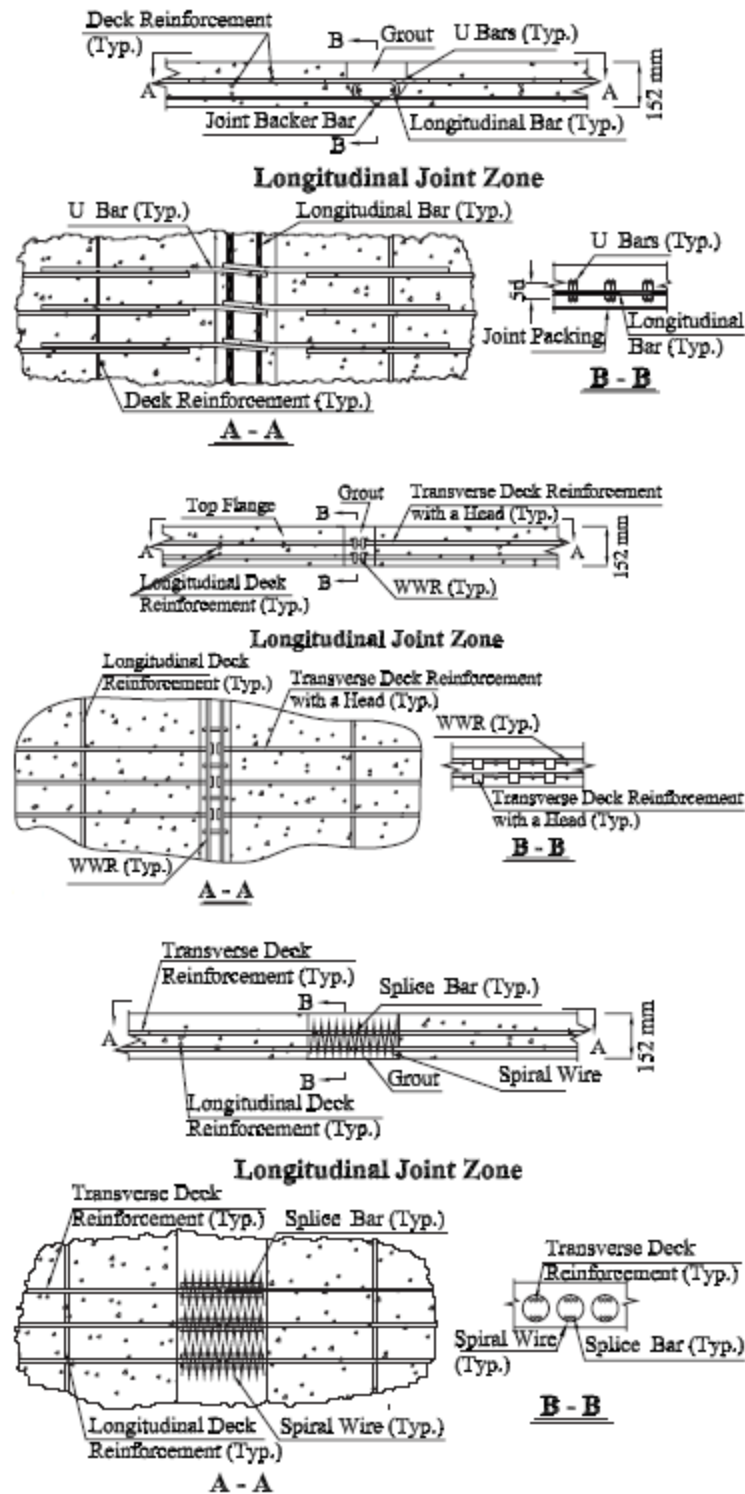


Figure 2.1: Recommended joint details (Li, Ma, Griffey, & Oesterle, 2010)

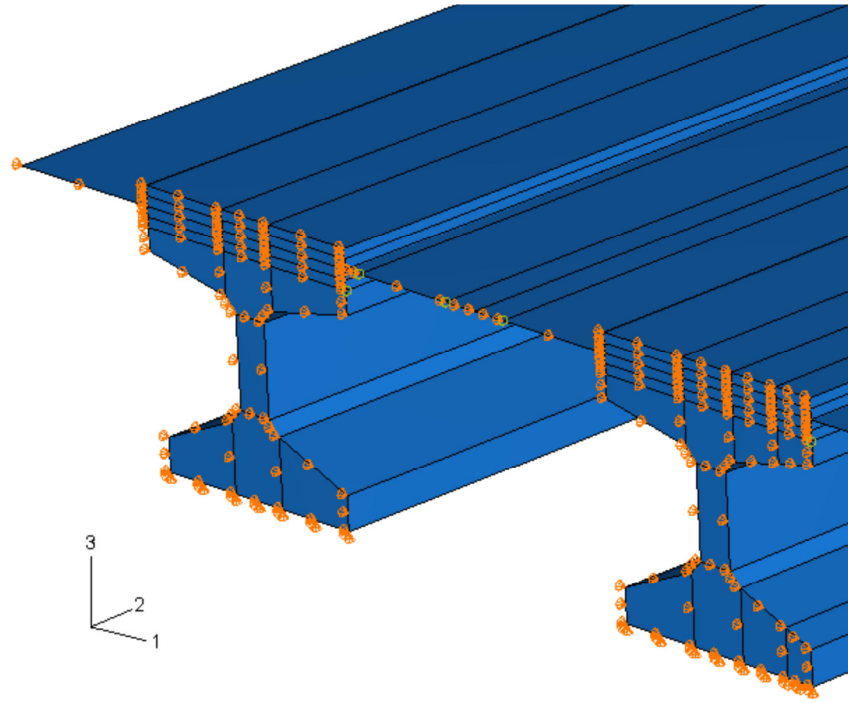


Figure 2.2: Finite element model (Li, et al., 2010)

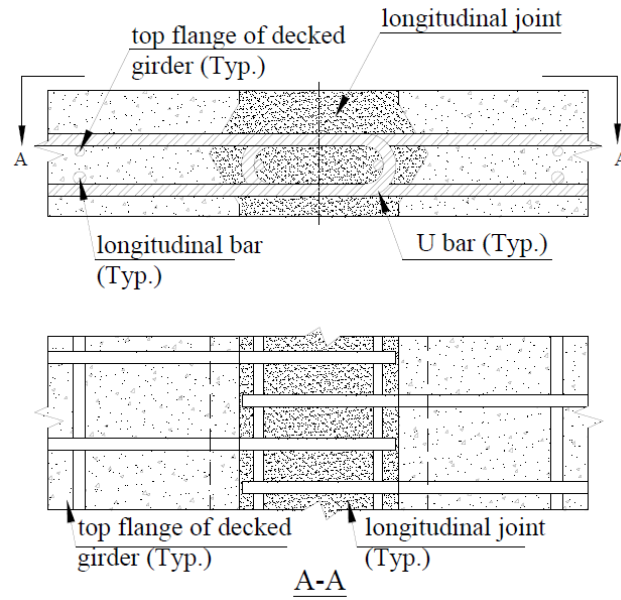


Figure 2.3: Proposed U-bar connection detail (French, et al., 2011)



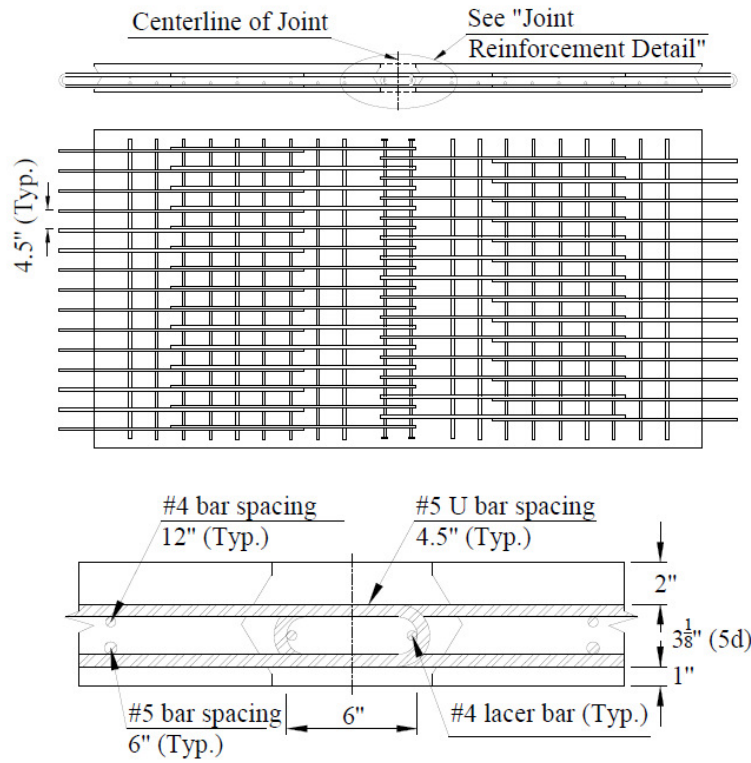


Figure 2.4: Large scale specimen dimensions (French, et al., 2011)



Figure 2.5: Large scale specimens prior to pour (French, et al., 2011)



Figure 2.6: Large scale specimens after pour (French, et al., 2011)



Figure 2.7: Welded plate detail (Gergely, Overcash, Mock, Clark, & Bailey, 2007)

## **CHAPTER III**

### **INVESTIGATION OF LONGITUDINAL JOINTS BETWEEN PRECAST PRESTRESSED DECK BULB TEE GIRDERS USING LATEX MODIFIED CONCRETE**

#### **3.1 EXPERIMENTAL PROCEDURE**

##### **3.1.1 Selection of Joint Detail**

A joint detail was selected for further testing based on results from the literature review. The criteria used for selection of the joint were moment capacity, shear capacity, ease of construction, and crack resistance. The welded metal plate connection detail currently in widespread use in the Pacific Northwest was eliminated due to concerns of excessive cracking at service loads. This connection is known to adequately resist shear, however it is poor in moment resistance. Also, typical spacing of the welded plates is five feet on center, leading to additional cracking between the connectors as well.

Multiple joint details were recommended by the recent studies conducted at UT-Knoxville as part of NCHRP 10-71 (French, et al., 2011). A survey of contractors and designers was first conducted where several potential details were presented. The respondents were asked about the constructability, reliability, and durability of each detail. The details which were most highly rated were the headed bar and U-bar details. When tested in small scale laboratory testing, both of these details demonstrated similar capacity in flexure as well as

shear, and had superior crack control to the welded plate detail. The U-bar detail was chosen for further large scale testing due to its better constructability. When placed in the field, the U-bars would form a cage which aided in placement of the longitudinal rebar.

This U- bar detail consists of interlaced U-bars which protrude from a shear key formed into the edges of each slab specimen. The U-bars are set 6 inches on center, so following placement the interlocked U-bars are 3 inches on center. Two #4 headed bars are then threaded longitudinally through the meshed U-bars. Schematics of the joint detail can be found as Figures 3.1 and 3.2.

### **3.1.2 Test Specimens**

Two large scale slab specimens were fabricated for this test. The specimens were designed to represent the deck portion of two adjacent deck bulb tee girders which would be connected through a longitudinal joint as part of a full-scale bridge. Both slabs were identical in size, at 6 feet long, 6 feet wide, and 8 inches thick. The deck thickness was chosen to be consistent with typical bridge decks in South Carolina. Specimen dimensions and reinforcing details can be seen in Figures 3.3 and 3.4. The reinforcing was designed to adhere to the SCDOT Bridge Design Manual and with standard bridge design practice in order to better correspond to real world conditions. The slab reinforcing which functioned as the longitudinal bridge reinforcing was designed at 12 inches on center both top and bottom. The reinforcing that functioned as transverse reinforcing and also contained the U-bars was laid out at 6 inches on center, top and bottom. Shear keys with U-bars were formed on both sides of the slabs, to allow for two tests on each specimen if necessary. The U-bars on each side were spliced with straight rebars in the center of the slab. All slab reinforcement was A706 Grade 60 #5 bars. Clear

cover for the rebars was designed to be 2 inches on top, and 1.5 inches on the bottom. This is slightly less than the typical 2.5 inches recommended in the SCDOT Bridge Design Manual (SCDOT, 2006), but was necessary to meet the minimum bend diameter of the U-bars as given in ACI 318 (ACI, 2011). The design strength of the concrete for the slabs was 6,000 psi. The mix design can be found in Table 3.1.

The forms were constructed of standard pine lumber and plywood. The shear key detail was formed from one inch foam board, with holes cut through the lumber and foam board to allow for protrusion of the U-bars. The interior of the forms were then sprayed with form release compound, and the slab concrete was poured on July 25, 2013. The forms were built in the USC structures laboratory, and a ready-mix concrete truck was driven into the lab in order to perform the pour in a climate controlled area. The measurements for slump and air content were 5 inches and 2.5%, respectively. Compressive strength data can be found in Table 3.2. The concrete was moist cured under wet burlap and plastic for 14 days. Following the initial cure, the forms were stripped and the slabs were cured for an additional 14 days for a total of 28 days. Figures 3.5 through 3.10 depict the specimens before and after casting and curing.

### **3.1.3 Closure Pour Material**

The closure pour material was selected from several candidates based on bond strength, tensile strength, and relative frequency of use in SCDOT applications. Previous studies had used various high performance concrete and grout mixtures, each approximately 10,000 psi in strength. These mixtures displayed good performance in ultimate strength and crack control. In order to further enhance crack control, a product with higher bond strength and ductility was desired, as well as one which was regularly used by bridge

contractors in South Carolina. Latex modified concrete was chosen based on these criteria. The latex modifier used was Styron Mod A/NA, which is pre-approved for use by the SCDOT, and exhibited the desired properties for this application. Three test LMC mixes were then designed to match the slab concrete strength of 6,000 psi. Each test batch included Eclipse<sup>®</sup> 4500 shrinkage reducing admixture to reduce cracking due to drying shrinkage.

The initial test mix (CPTM-1) demonstrated a higher than expected slump due to the water reducing properties of the latex modifier. The second test mix (CPTM-2) reduced the slump slightly however still had excess workability. The third test mix (CPTM-3) used Type III cement and had a 5" slump, meeting the targeted value. This mix design was then used as the closure pour material. The mix designs can be found in table 3.3. Properties of the closure pour batch can be found in table 3.4.

#### **3.1.4 Joint Construction**

After the 28 day cure period of the slabs, both specimens were lifted into place on reaction stands, so that the U-bars interlocked. Two #4 headed lacer bars were threaded through the interlocked U-bars longitudinally down the joint. Formwork was then constructed and clamped in place on either end and beneath the joint. To prevent sagging following concrete placement, cribbage and two jacks were placed beneath the formwork for support. Once in place, the joint face was sandblasted to remove carbonation and provide fresh concrete to enhance bonding of the LMC. Figures 3.10 through 3.13 depict joint construction steps.

The latex modified concrete was mixed and placed on September 13, 2013. Concrete was mixed using a Stone<sup>®</sup> 95CF mixer, and was vibrated for consolidation

around the U-bars. Air content and slump tests were performed, and cylinders were taken for compressive strength and elastic modulus testing. Results of these tests can be found in Table 3.4. Following placement, the concrete was wet cured in place using water-soaked burlap for 14 days, following which the forms were stripped and the test frame constructed. Figures 3.14 through 3.16 display the joint following the closure pour.

Six shrinkage specimens were cast from the closure pour material according to ASTM C157 to determine the effectiveness of the shrinkage reducing admixture when used in latex modified concrete. Figures 3.17 and 3.18 display the shrinkage specimens and results of the testing.

### **3.1.5 Experimental Setup and Instrumentation**

The specimens were tested in combined flexure and shear loading in the USC Structures Laboratory. The specimens were simply supported with a 72 inch span. A test frame was constructed around the specimens where a 110 kip actuator was mounted to apply the load. The actuator was attached to a 3 foot spreader beam, which transferred the load to two separate load points along the joint equally to apply a strip load parallel to the joint. Both load points were positioned 1 foot from the center line of the joint, producing the desired shear and moment as discussed in section 3.1.6. The test setup is shown in figure 3.19, and diagrams of the test frame are presented in figures 3.20 and 3.21.

The specimens were equipped with linear displacement gauges at the supports and at either end of the joint to detect settlement of the supports and displacement of the joint center. A load cell was used to determine the load applied by the actuator to the spreader beam.

### **3.1.6 Test Procedure**

Loads for the experimental test were developed after review of the finite element study conducted in the NCHRP 10-71 project. The specimen was first subject to a fatigue loading program which was divided into four cycles, F1, F2, F3, and F4. Each fatigue cycle consisted of 500,000 load cycles for a total of 2,000,000 load cycles. The actuator was programmed to cycle between a minimum load of 4.4 kips and a maximum load of 25 kips. The load cycles were applied at a rate of 1.5 Hz. The minimum and maximum loads corresponded to the shear forces resisted by the joint under the fatigue modified HL-93 live loading according to the finite element study completed as part of NCHRP 10-71 (French, et al., 2011). The minimum shear force was due to differential camber leveling and was assumed to be constant at 0.5 kips/ft. The maximum shear force was due to the HL-93 fatigue load plus the camber leveling force, for a total of 2.84 kips/ft. The shear force along the joint was found to vary significantly based on longitudinal position of the bearing pad. This led to a shear concentration toward the center of the joint in excess of the average shear per unit length of the joint.

The fatigue loading was paused at 500,000 cycle intervals and a service level overload was performed. A 46.9 kip force was applied by the actuator which corresponded with a peak shear of 5.34 kips/ft. This was the shear carried by the joint under the unfactored AASHTO HL-93 live load in the finite element model conducted as part of NCHRP 10-71 (French, et al., 2011).

Upon completion of the fatigue loading program, the influence of cracking on the water tightness of the joint was investigated via a ponding test. Prior to commencing fatigue loading, a dike was constructed around the joint area using standard 2x4 lumber



and Power Stick<sup>®</sup> adhesive to form the watertight seal. Water was then poured inside the dike to a depth of 2 inches above the concrete, so that the joint area was fully submerged. Observations were then made to determine if water was leaking through the joint during fatigue testing as a result of crack development. The dike and ponding test is presented in figure 3.22.

## **3.2 RESULTS AND DISCUSSION**

The main experimental results are introduced and discussed in this section. Results related to shrinkage, cracking, and behavior under loading are discussed.

### **3.2.1 Shrinkage**

Six shrinkage specimens were cast from the closure pour material and were tested to determine the shrinkage behavior of the closure pour material and the effectiveness of the shrinkage reducing admixture. Length measurements were taken using a comparator with a 10 inch gage length at intervals recommended by ASTM C157. Initial measurements were made 24 hours following casting, after which the specimens were placed in a lime saturated water bath for 28 days to cure. Following the curing period, another measurement was taken, and the specimens were placed on a rack to air dry.

Measurements were then taken at 7, 14, 21, and 28 days from the initial cure period.

Length change from 0.02 to 0.025% at 28 days was observed.

### **3.2.2 Cracking**

The slab specimen was visually inspected during the fatigue testing phase for the presence of cracks. No cracking was detected as a result of the fatigue or service level loading during the testing. Figures 3.23 and 3.24 show the joint following the conclusion of fatigue testing.

A ponding test was also performed following the fatigue loading phase to confirm whether or not there were cracks present which were too small for visual detection. Water was allowed to stand on top of the joint for 4 days, during which time no water was detected leaking through the joint. Water was seen discharging from one end of the joint, indicating crack development at the interface between the existing concrete and the closure pour. The location of the crack in the compressive zone of the joint suggests that the crack could be a result of inadequate consolidation during placement of the LMC or drying shrinkage causing the closure pour to pull away from the existing concrete. Ultimately, it is probable that no cracking occurred in the joint as a result of external loads applied during the fatigue testing phase. Lack of water discharging through the vertical length of the joint also indicates the absence of any through cracks. Figure 3.25 displays the discharge from the end of the joint.

### **3.2.3 Specimen Behavior**

Average deflection under fatigue and service level loading was approximately 0.6 and 2 mm (0.024 and 0.079 inches) respectively. Throughout the testing regimen, the joint was able to resist the applied loads without any signs of distress.

The specimen underwent permanent deformation over the course of the fatigue loading phase. This deformation increased during the first two load cycles, F1 and F2, but began decreasing during F3 and F4. Load vs. displacement charts can be seen as figures 3.26 through 3.31 and permanent deformation can be seen in table 3.5. Based on the data, it was shown that at fatigue and service level loads no significant permanent deformation occurred in the slab specimen. This result is consistent with the slab behavior reported in NCHRP 10-71 (French, et al., 2011), and indicates that the joint is capable of transferring

and resisting service and fatigue level loads without sustaining damage over the lifespan of the bridge.

One possible reason for residual slab deformation initially increasing and then decreasing during fatigue loading is strengthening of the LMC closure pour concrete as it cured, causing increasing stiffness of the joint. Another possible explanation is strain redistribution of the reinforcing steel, mobilizing more cross sectional area and thereby reducing the effective stresses resisted by the rebar.

### **3.3 CONCLUSION**

The absence of longitudinal cracks developing in the tensile zone of the joint indicate the capability of LMC to resist crack formation and debonding from existing concrete. This result in conjunction with insignificant levels of permanent deformation under cyclic loading demonstrates the adequacy of the joint to transfer and resist service level shear and moment in precast bridge systems without sustaining permanent damage and loss of strength over the life span of the bridge.

Table 3.1: Slab specimen concrete mix proportion

	Slab Concrete
w/c ratio	0.337
Coarse Aggregate (lb/yd <sup>3</sup> )	1728.6
Fine Aggregate (lb/ yd <sup>3</sup> )	1143.4
Super Plasticizer (fl oz/yd <sup>3</sup> )	45.6
Retarder (fl oz/yd <sup>3</sup> )	14.9
Air Entrainment (fl oz/yd <sup>3</sup> )	1.5

Table 3.2: Compressive strength of slab concrete

	Compressive Strength (psi)	Modulus of Elasticity (psi)
7-day	5680	-
14-day	6264	-
21-day	6240	-
28-day	6466	-
56-day	7142	4.9x10 <sup>6</sup>

Table 3.3: Mix designs of closure pour test batches

	CPTM-1	CPTM-2	CPTM-3	CP
w/c ratio	0.33	0.33	0.28	0.28
Coarse Aggregate (lb/yd <sup>3</sup> )	1720	1260	1260	1260
Fine Aggregate (lb/yd <sup>3</sup> )	1048	1505	1596	1596
Latex Modifier (lb/yd <sup>3</sup> )	208	208	208	208
Air Entrainment (fl oz/yd <sup>3</sup> )	1.5	1.5	1.5	1.5
Super Plasticizer (fl oz/yd <sup>3</sup> )	24.4	0	0	0
Water Reducer (fl oz/yd <sup>3</sup> )	15	15	15	15
Shrinkage Reducer (lb/yd <sup>3</sup> )	11.55	11.55	11.55	11.55

Table 3.4: Closure pour concrete properties

	Compressive Strength (psi)
7-day	4442
14-day	5159
21-day	5343
28-day	5441
56-day	6247

Table 3.5: Residual specimen displacement

Cycles	Residual Displacement mm (in)
500,000	0.619 (0.024)
1,000,000	0.942 (0.037)
1,500,000	0.919 (0.036)
2,000,000	0.815 (0.032)

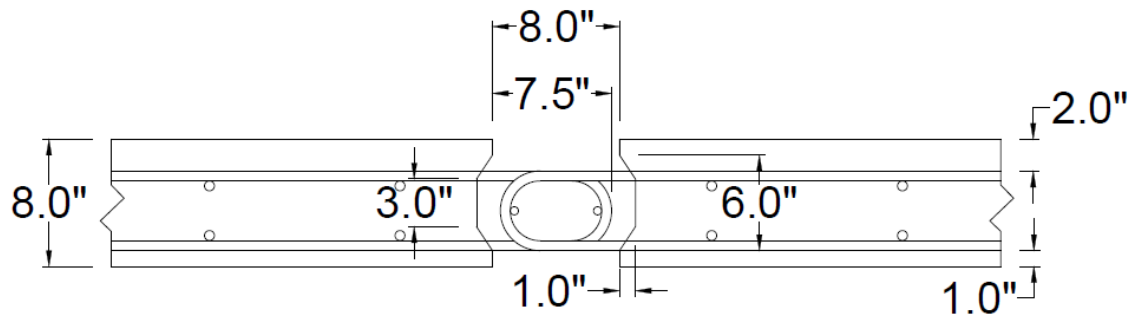


Figure 3.1: Section view of longitudinal joint detail

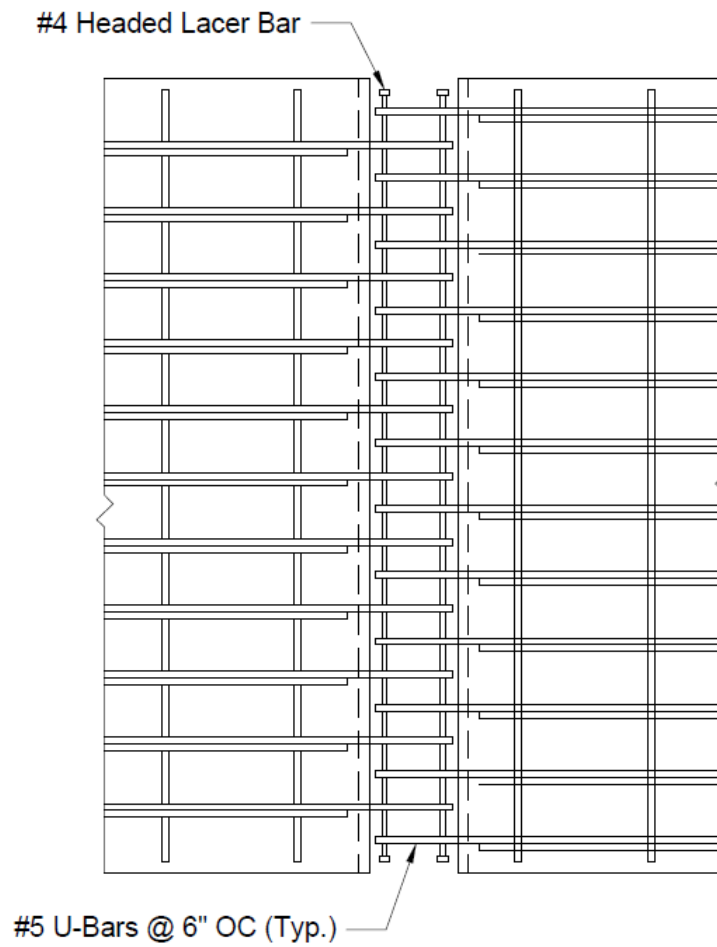


Figure 3.2: Plan view of longitudinal joint detail

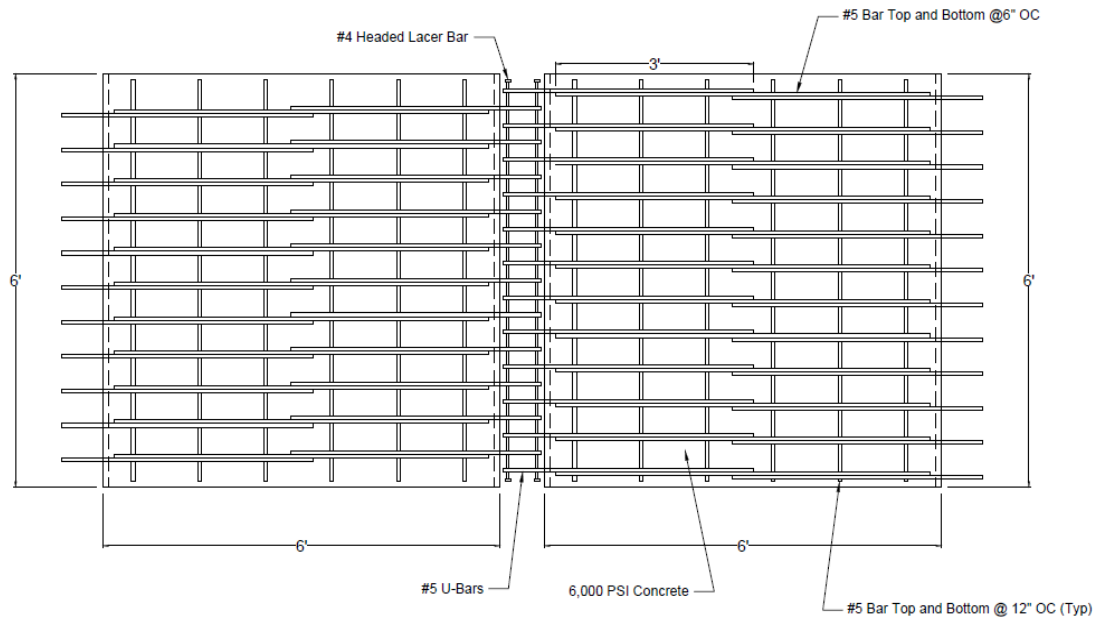


Figure 3.3: Plan view of test specimen

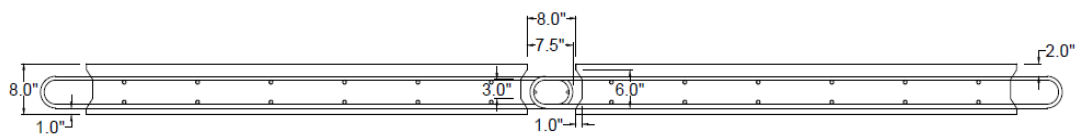


Figure 3.4: Elevation view of test specimen





Figure 3.5: Specimen formwork with foam board for shear key

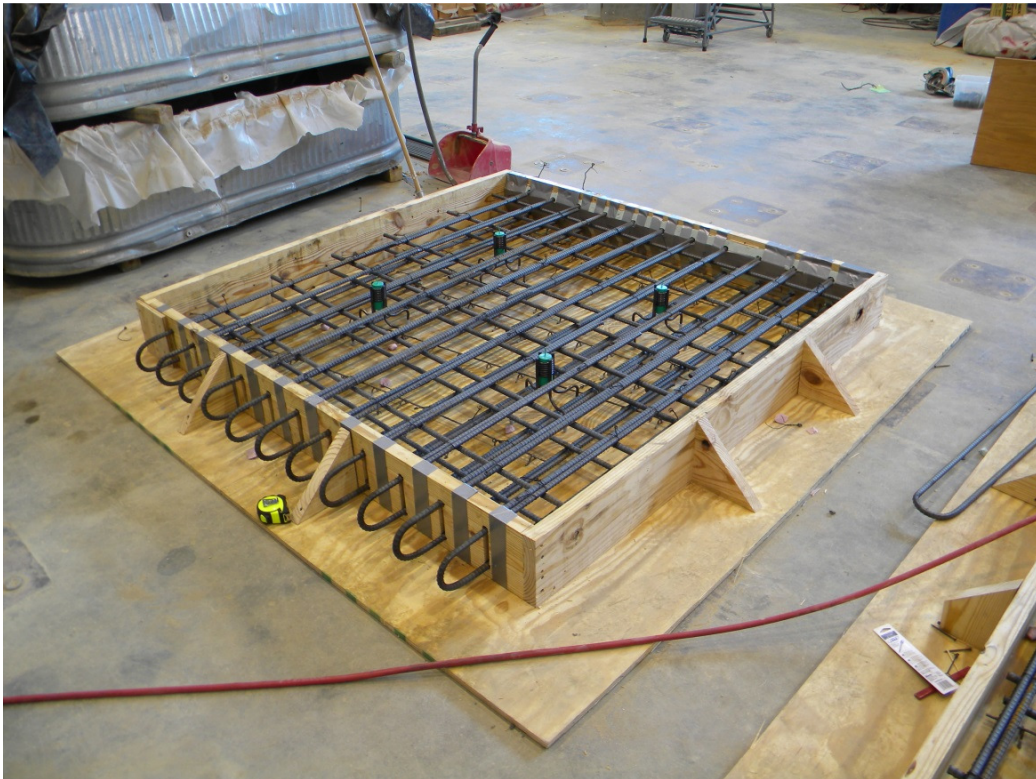


Figure 3.6: Specimen formwork with tied rebar



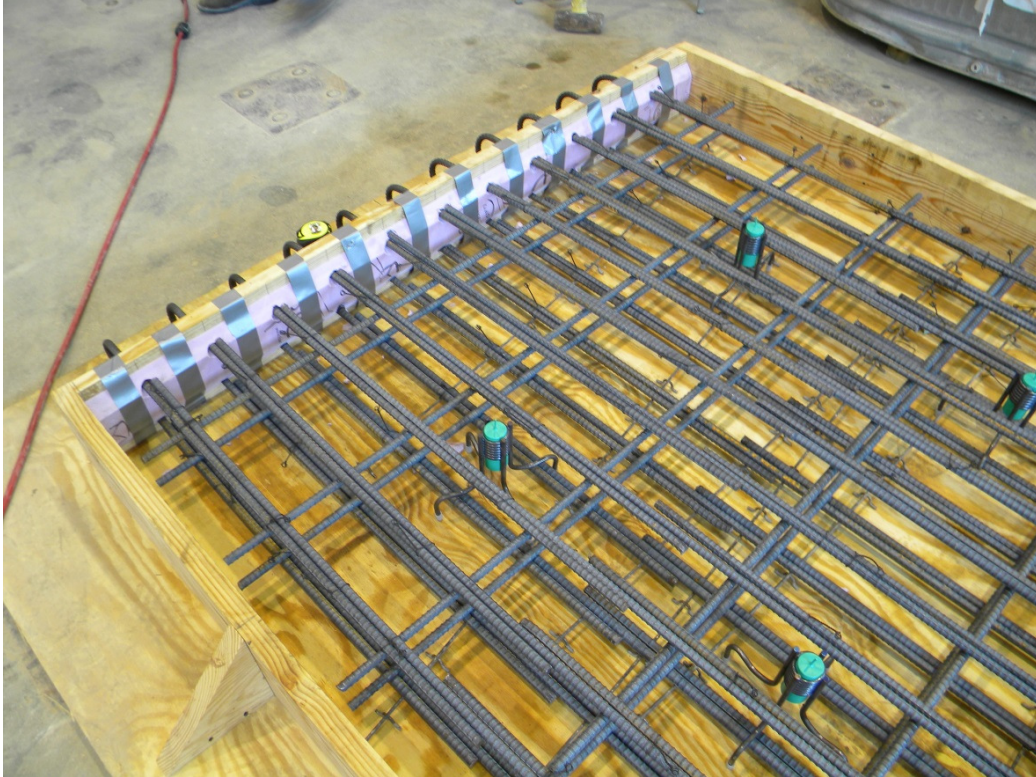


Figure 3.7: View of tied rebar with lift inserts



Figure 3.8: View of both specimens with rebar





Figure 3.9: Specimens being moist cured



Figure 3.10: Specimen after casting and curing





Figure 3.11: Specimens set in place to form the joint prior to sandblasting



Figure 3.12: Joint formed with #4 headed bars in position following sandblasting





Figure 3.13: View of completed joint prior to pour



Figure 3.14: Joint following closure pour





Figure 3.15: End view of joint



Figure 3.16: Burlap and plastic used for curing joint



Figure 3.17: Shrinkage specimens

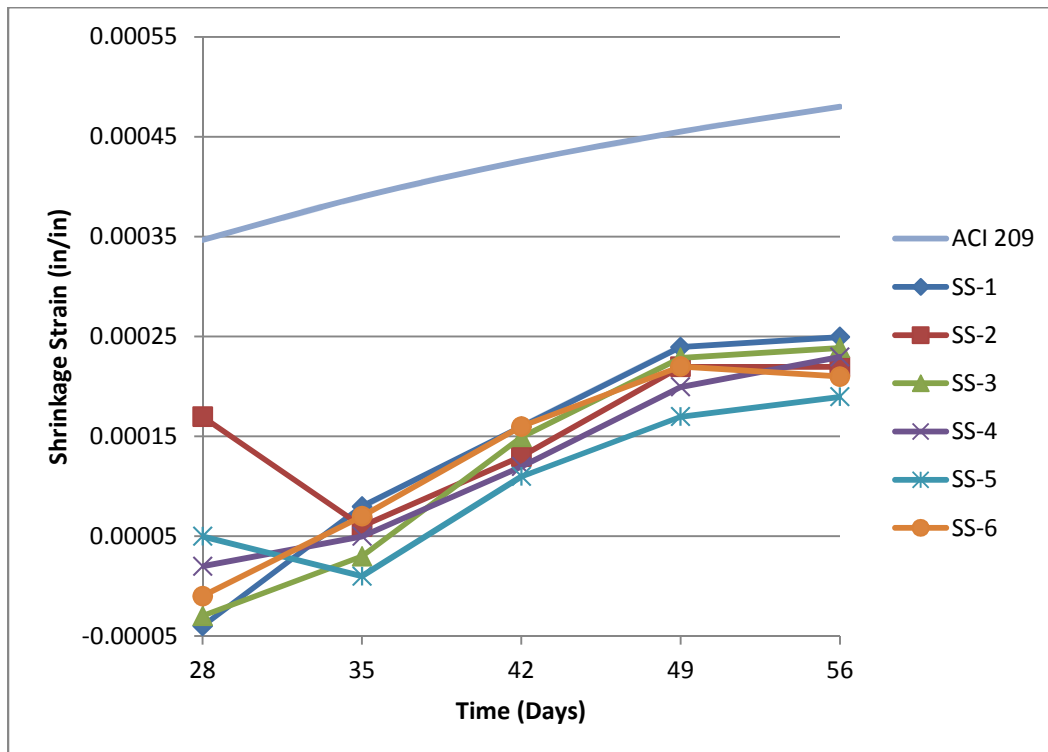


Figure 3.18: Shrinkage test results



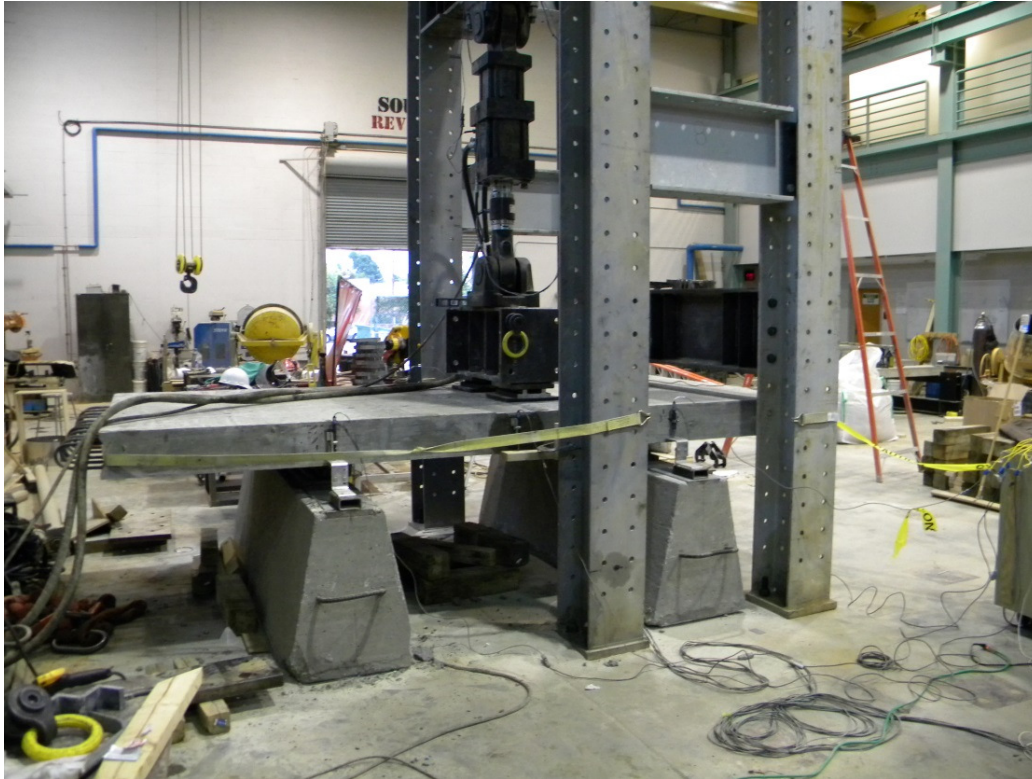


Figure 3.19: View of test set up

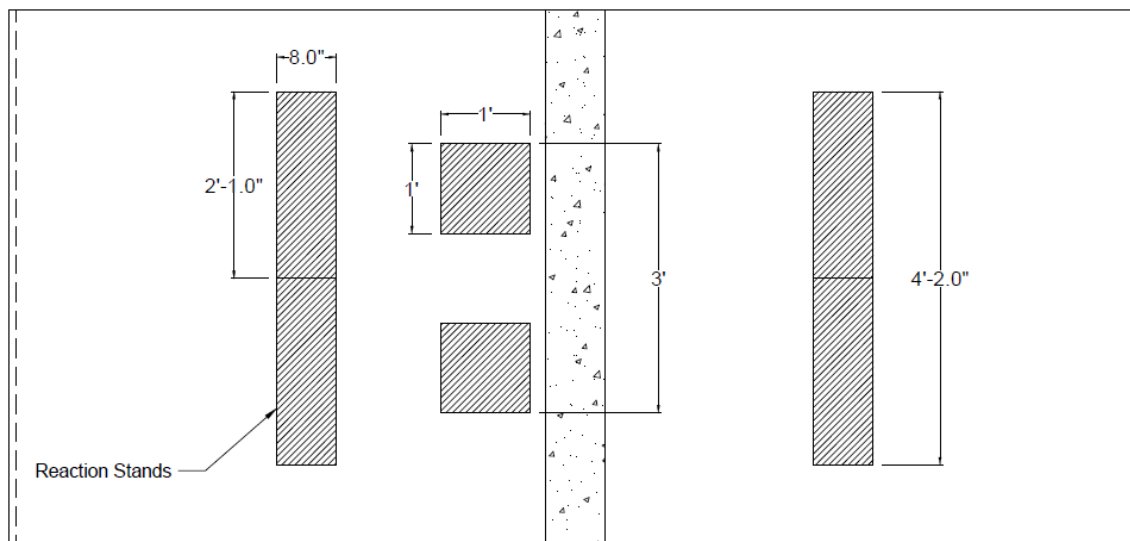


Figure 3.20: Plan view of test set up



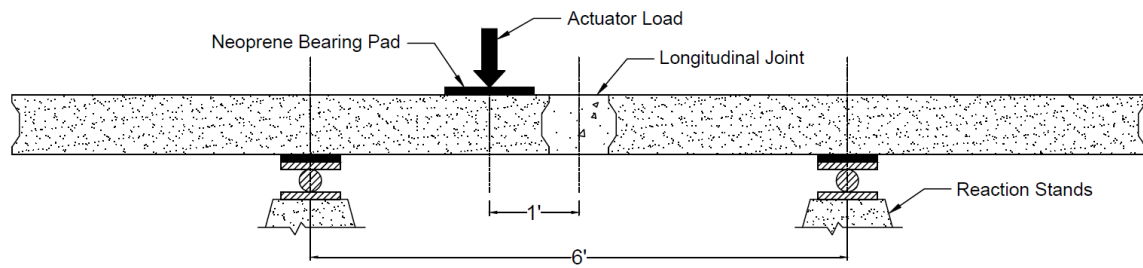


Figure 3.21: Elevation view of test set up



Figure 3.22: Joint condition following fatigue testing



Figure 3.23: Underside of joint after fatigue loading

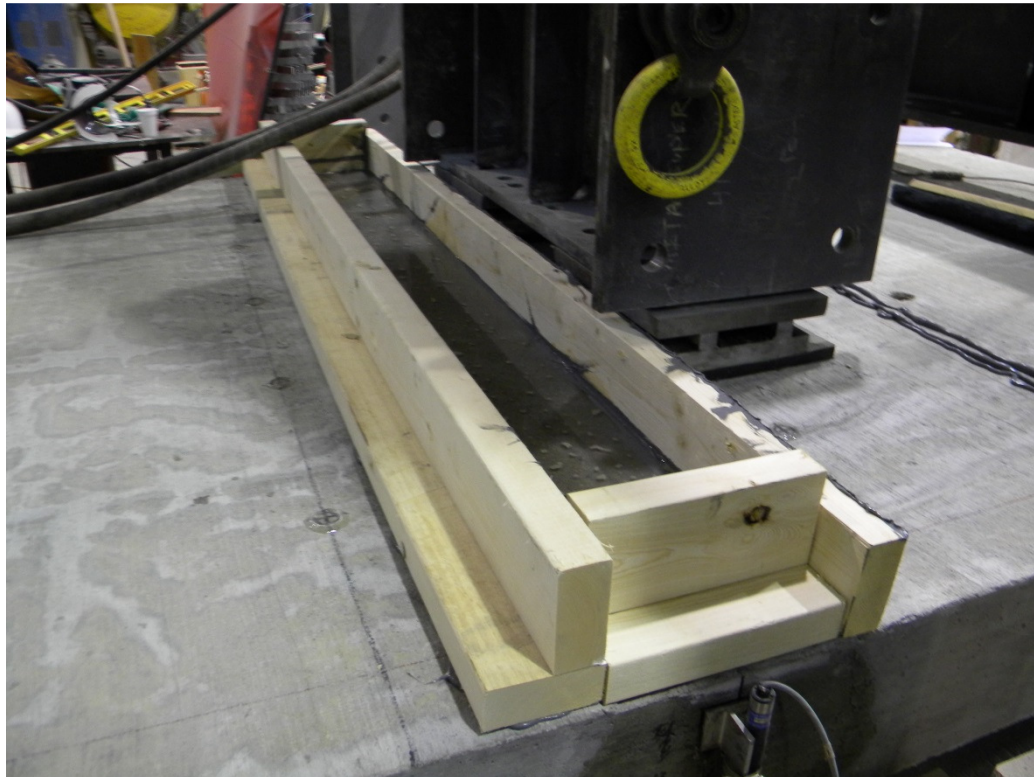


Figure 3.24: View of ponding test



Figure 3.25: Leaking at end of joint

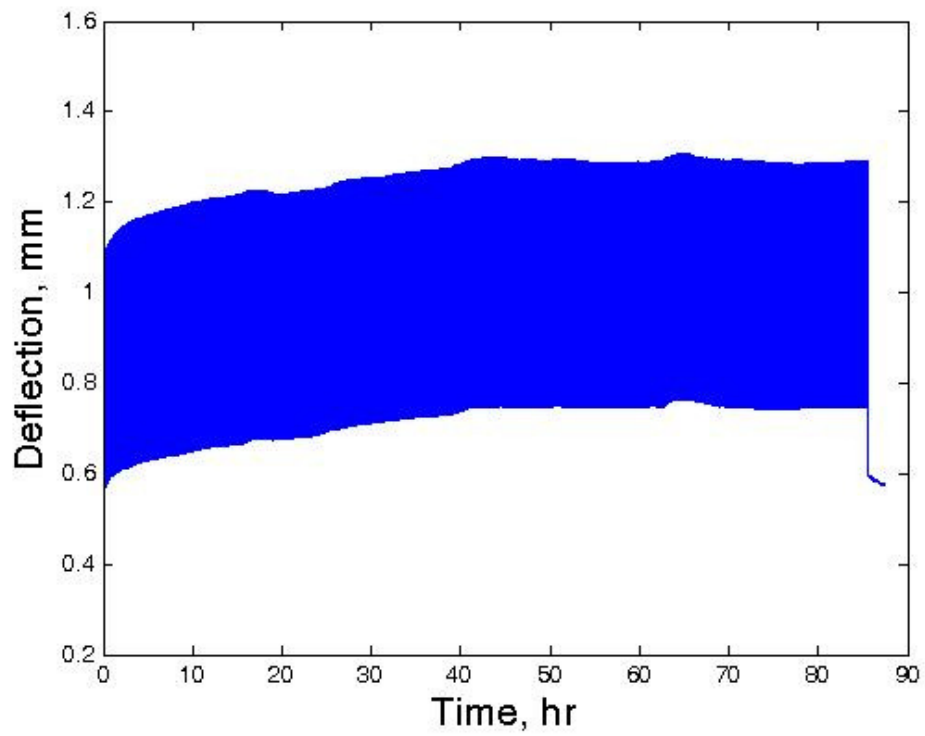


Figure 3.26: Fatigue cycle F1 deflection over time



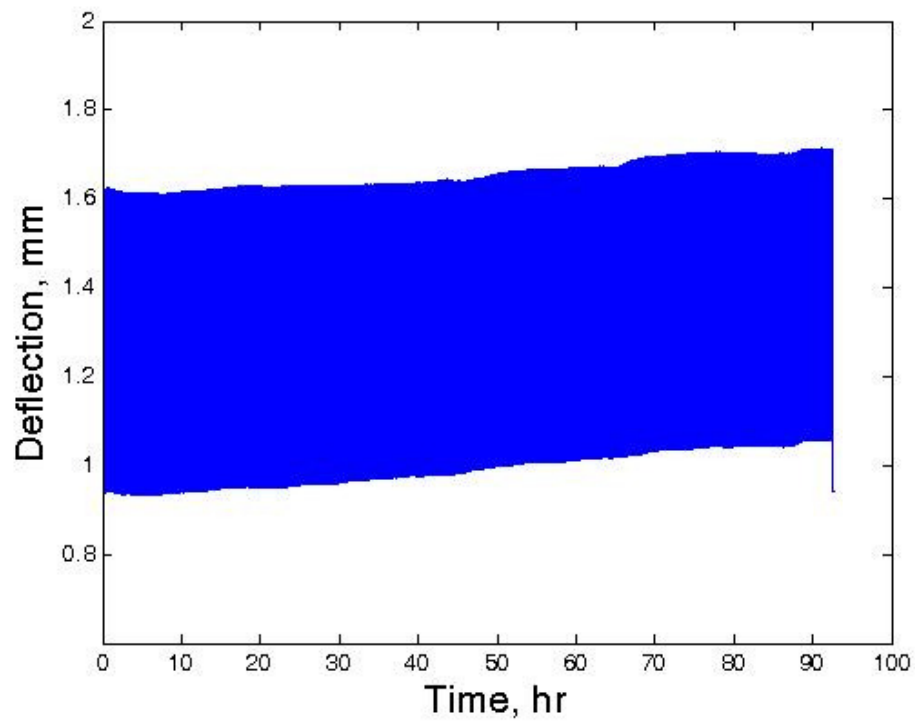


Figure 3.27: Fatigue cycle F2 deflection over time

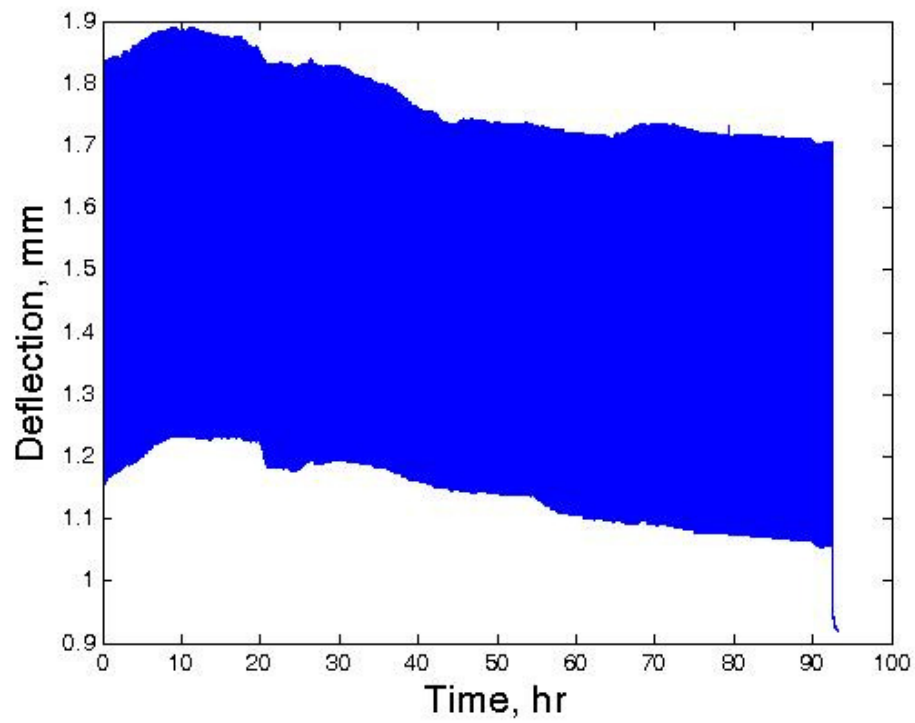


Figure 3.28: Fatigue cycle F3 deflection over time

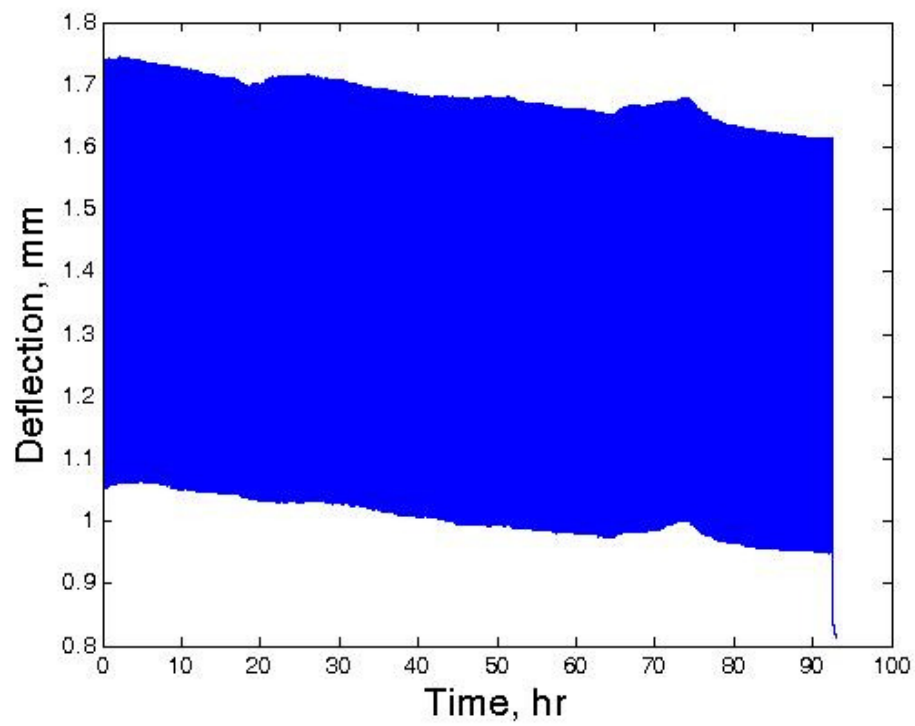


Figure 3.29: Fatigue cycle F4 deflection over time

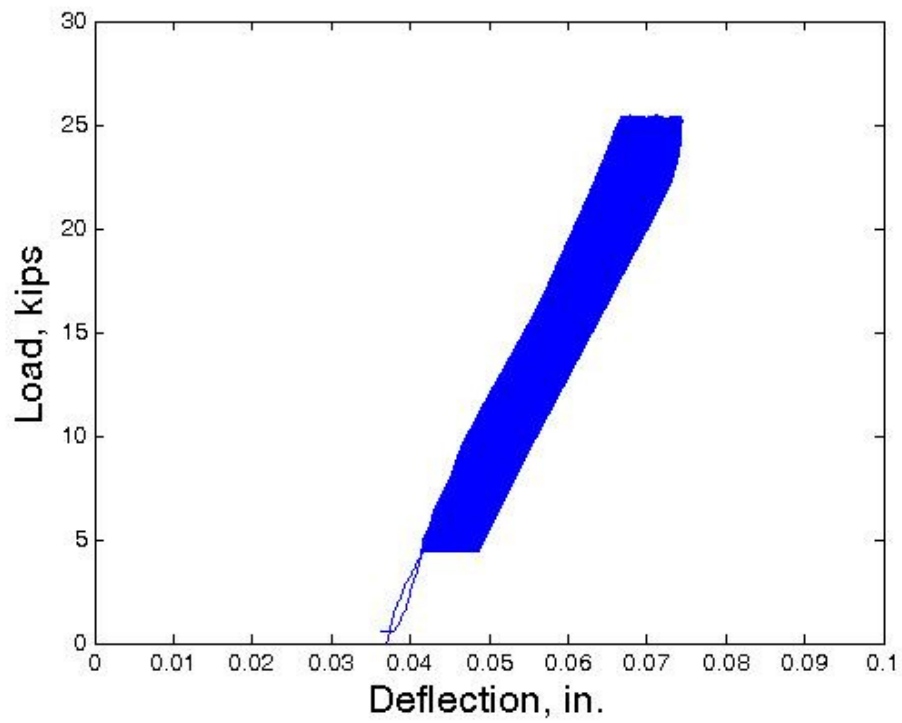


Figure 3.30: Load vs. deflection for fatigue cycle F3

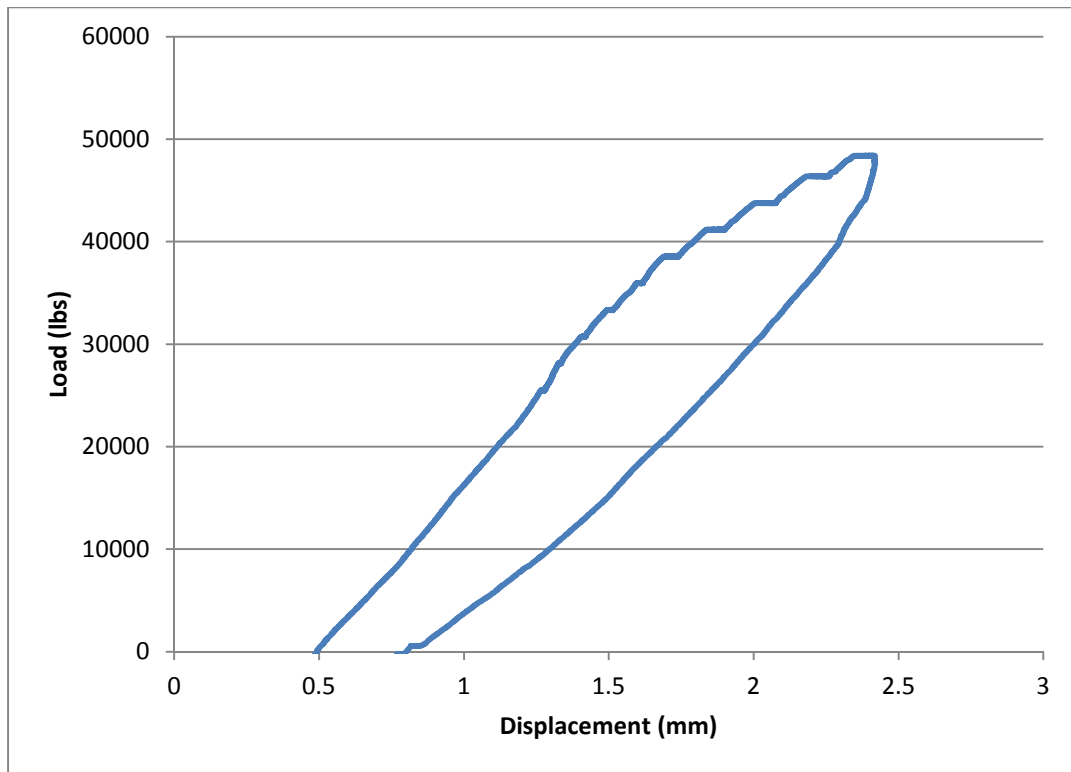


Figure 3.31: Load vs. deflection for service level overload 1

## **CHAPTER IV**

### **SUMMARY AND CONCLUSIONS**

#### **4.1 SUMMARY**

Current practice for construction of the longitudinal joint between precast deck bulb tee bridge girders typically results in excessive cracking, resulting in durability concerns. In previous studies, it was shown that the primary through cracks that develop in these joints occur at the interface between the existing deck concrete and the closure pour. Latex modified concrete exhibits higher bond strength and ductility than standard concrete, and is therefore capable of reducing crack formation at the interface.

Two large scale slab specimens were cast and joined using latex modified concrete as the closure pour material. These specimens were then subjected to fatigue loading of 2,000,000 cycles at 1.5 Hz. The load varied between 4.4 kips and 25 kips to produce the shear and moment which was calculated in the finite element study conducted as part of NCHRP 10-71 (French, et al., 2011). At 0.5 million cycle intervals, the fatigue loading was paused and a service level overload was applied at 46.9 kips. During the fatigue and service level loading, no visible cracking occurred. Following the last service loading, a ponding test was conducted. No water was seen penetrating through the joint, however a discharge was seen coming from a crack in the end of the joint in the compressive zone. It is possible that this crack developed as a result of shrinkage or inadequate consolidation during placement and not from external loading.

Deflection data also demonstrates that no significant permanent deformation occurred during the fatigue loading phase. This indicates that the U-bar detail and LMC formed a joint which is capable of transferring service level shear and moment between adjacent bridge girders without sustaining excessive damage and loss of strength.

## **4.2 CONCLUSIONS**

The U-bar joint detail displayed superior moment and cracking resistance when tested as part of NCHRP 10-71 (French, et al., 2011), however some cracking persisted at service level loading. Since these cracks formed at the interface between the existing concrete and the closure pour, a material with higher bond strength was proposed to counter this effect. Crack formation during the fatigue testing of this study could not be visually detected, and no through cracking appears to have occurred based on the results of the ponding test. Limited water discharge was seen at one joint end, however the crack permitting the flow developed in the compressive zone of the slab. This would indicate that the crack was possibly due to drying shrinkage or developed during placement of the closure pour concrete.

Due to the elimination of cracking in the tensile zone of the joint area as well as the performance of the joint in fatigue and service level loading, a joint system consisting of LMC and a U-bar reinforcing detail is recommended for use in longitudinal joints between deck bulb tee girders.

## **4.3 RECOMMENDATIONS AND FUTURE WORK**

Further fatigue loading of the joint will be conducted to reach a total of 2,850,100 cycles, matching the expected truck traffic over a typical bridge employing this type of



construction. The specimen will then be subjected to the CLT protocol as proposed by ACI Committee 437 to determine failure load and behavior of the specimen in failure.

A prototype bridge will also be constructed using rapid construction methods consisting of precast prestressed deck bulb tee girders. LMC can be used in the closure pour to determine the full scale behavior of the LMC/U-bar joint system when part of a bridge. Additional refinements to the detail include: removal of the #4 headed lacer bars, epoxy coated U-bars, bonding agents between the concrete and closure pour, and lightweight concrete decks. Additional specimens should be tested using these variations to determine if further performance and efficiency gains are possible.

## REFERENCES

- French, C., Shield, C., Klaseus, D., Smith, M., Eriksson, W., Ma, Z., . . . Chapman, C. (2011). *Cast-in-Place Concrete Connections for Precast Deck Systems*. Washington: National Cooperative Highway Research Program.
- Gergely, J., Overcash, G., Mock, J., Clark, C., & Bailey, K. (2007). *Evaluation of Design and Construction of HPC Deck Girder Bridge in Stanly County, North Carolina*. Charlotte: Department of Civil Engineering, University of North Carolina at Charlotte.
- Holland, R., Dunbeck, J., Lee, J., Kahn, L., & Kurtis, K. (2011). *Evaluation of a Highway Bridge Constructed Using High Strength Lightweight Concrete Bridge Girders*. Atlanta: Georgia Department of Transportation.
- Li, L., Ma, Z., & Oesterle, R. (2010). Improved Longitudinal Joint Details in Decked Bulb Tees for Accelerated Bridge Construction: Fatigue Evaluation. *Journal of Bridge Engineering*, 511-522.
- Li, L., Ma, Z., Griffey, M., & Oesterle, R. (2010). Improved Longitudinal Joint Details in Decked Bulb Tees for Accelerated Bridge Construction: Concept Development. *Journal of Bridge Engineering*, 327-336.
- Ma, Z., Chaudhury, S., Millam, J., & Hulsey, J. (2007). Field Test and 3D FE Modeling of Decked Bulb-Tee Bridges. *Journal of Bridge Engineering*, 306-314. Oesterle, R., & Elremaily, A. (2009). *Design and Construction Guidelines for Long-Span Decked Precast, Prestressed Concrete Girder Bridges*. Washington: National Cooperative Highway Research Program.
- SCDOT. (2006). *SCDOT Bridge Design Manual*. Columbia: South Carolina Department of Transportation.
- Zhu, P., & Ma, Z. (2010). Selection of Durable Closure Pour Materials for Accelerated Bridge Construction. *Journal of Bridge Engineering*, 695-704.
- ACI committee 318. (2008). Building Code Requirements for Structural Concrete (ACI 318-08). *American Concrete Institute*, Farmington Hills, MI.
- AASHTO. (2010). *Bridge Design Specifications, 5th Edition*, American Association of State Highway and Transportation Officials, Washington, DC.

ACI committee 209. (1992). Prediction of Creep, Shrinkage, and Temperature Effects in Concrete Structures (ACI 209R-92) (Reapproved 1997). *American Concrete Institute*, Farmington Hills, MI, 48 pp.

ACI committee 437. (2007). Strength Evaluation of Existing Concrete Structures (ACI 437-12) *American Concrete Institute*, Farmington Hills, MI, 48 pp.

## APPENDIX A

### ADDITIONAL FATIGUE AND SERVICE LEVEL TEST DATA

The remaining load and displacement data that were not previously displayed in Chapter III are presented here.

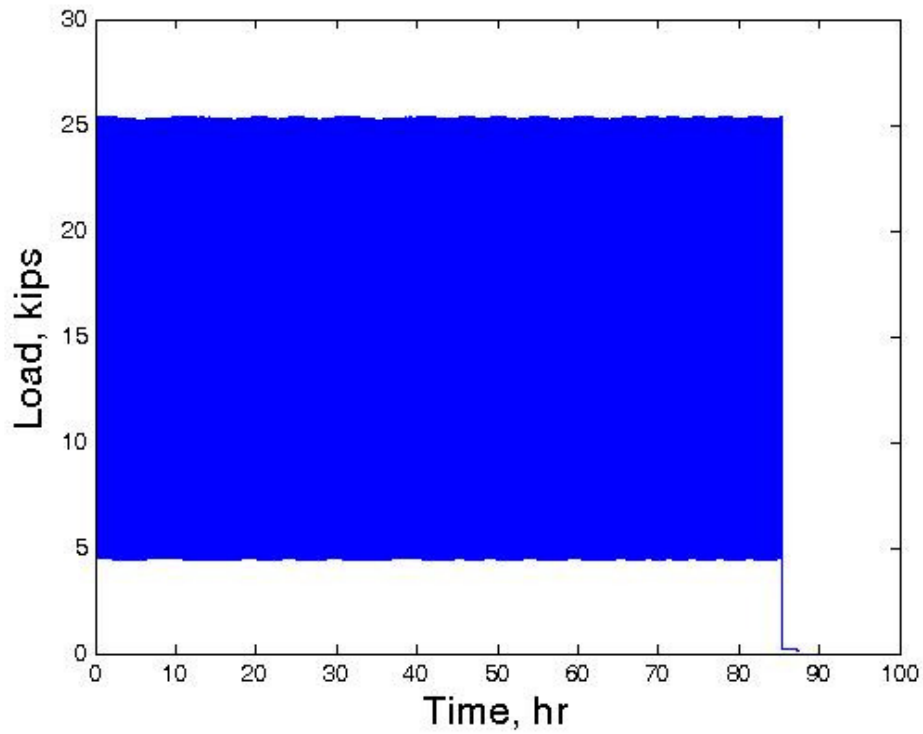


Figure A.1: F1 load versus time

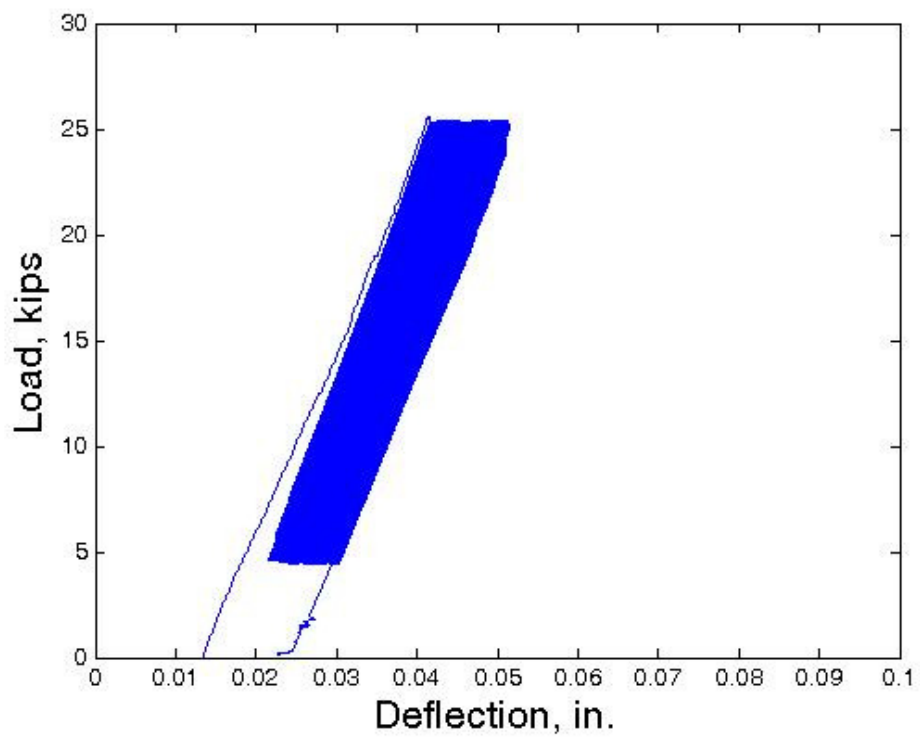


Figure A.2: F1 Load versus deflection

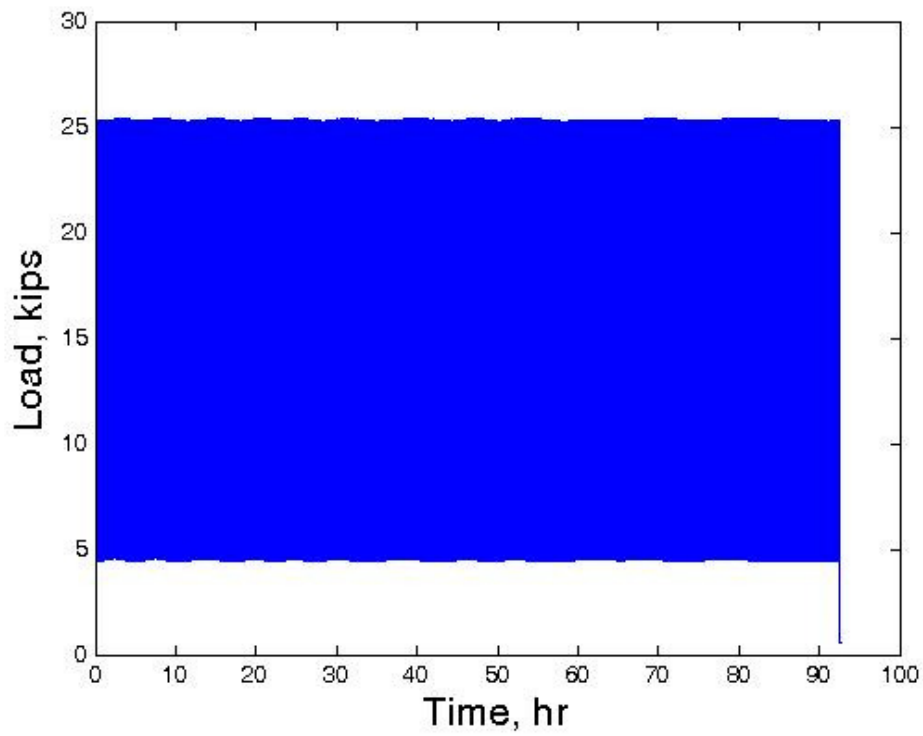


Figure A.3: F2 Load versus time

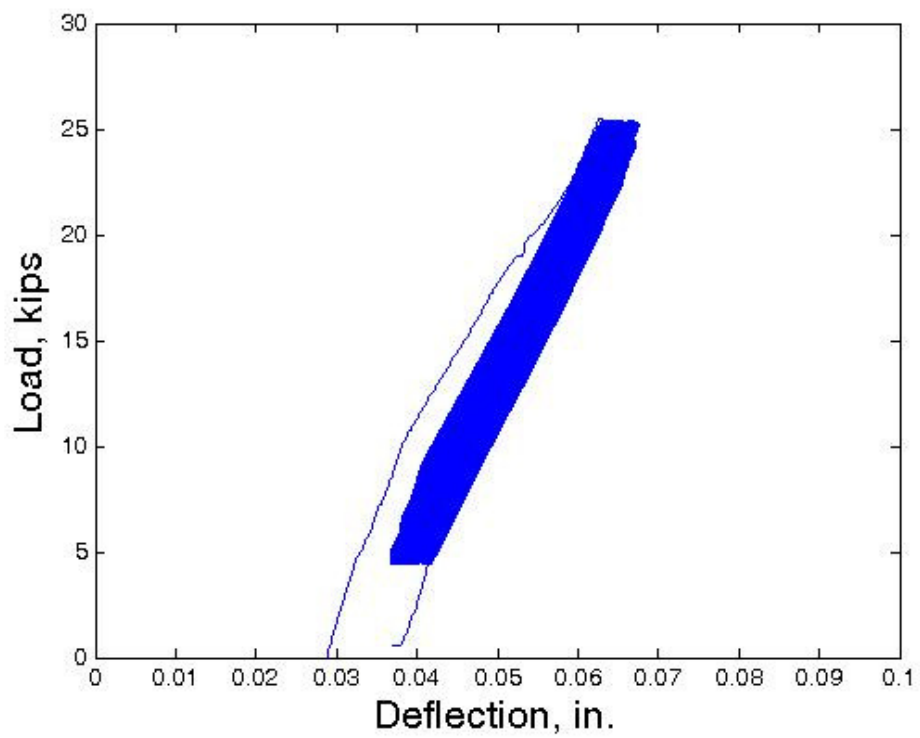


Figure A.4: F2 Load versus deflection

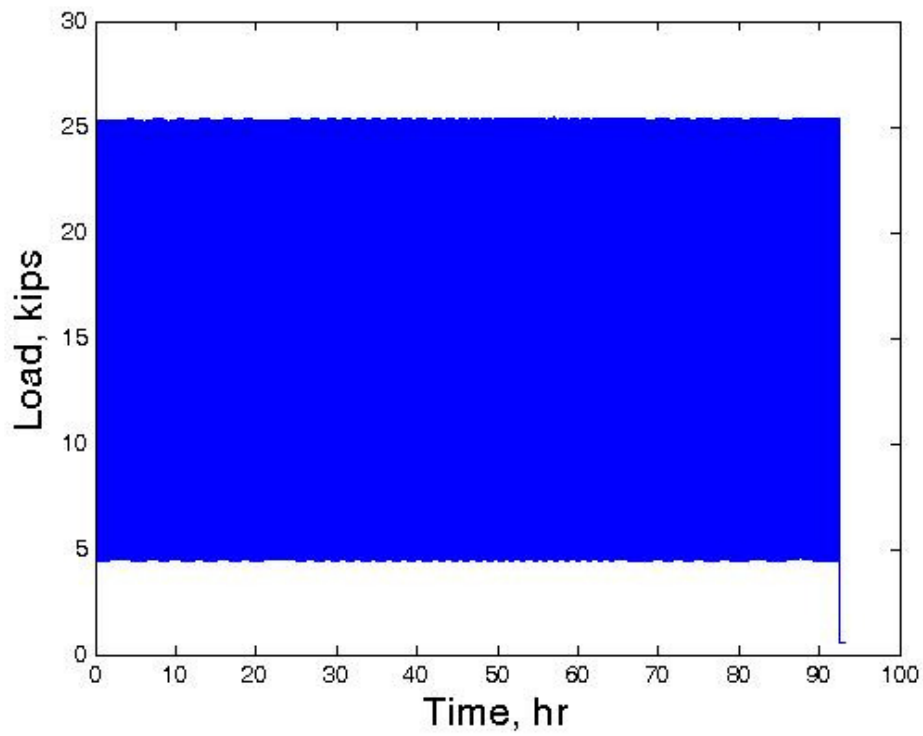


Figure A.5: F3 Load versus time

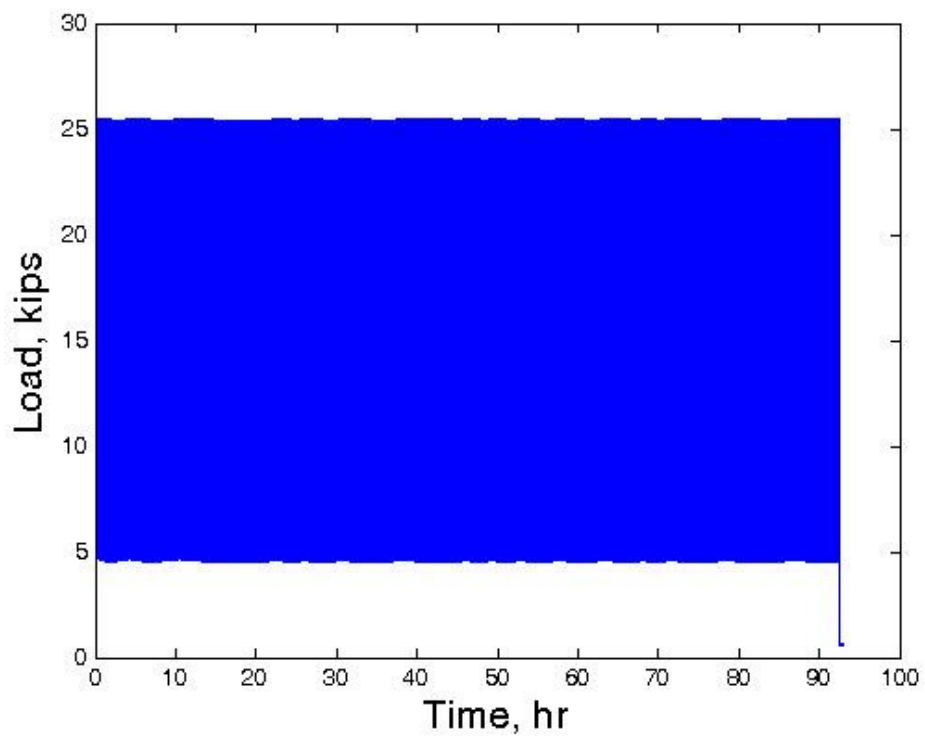


Figure A.6: F4 Load versus time

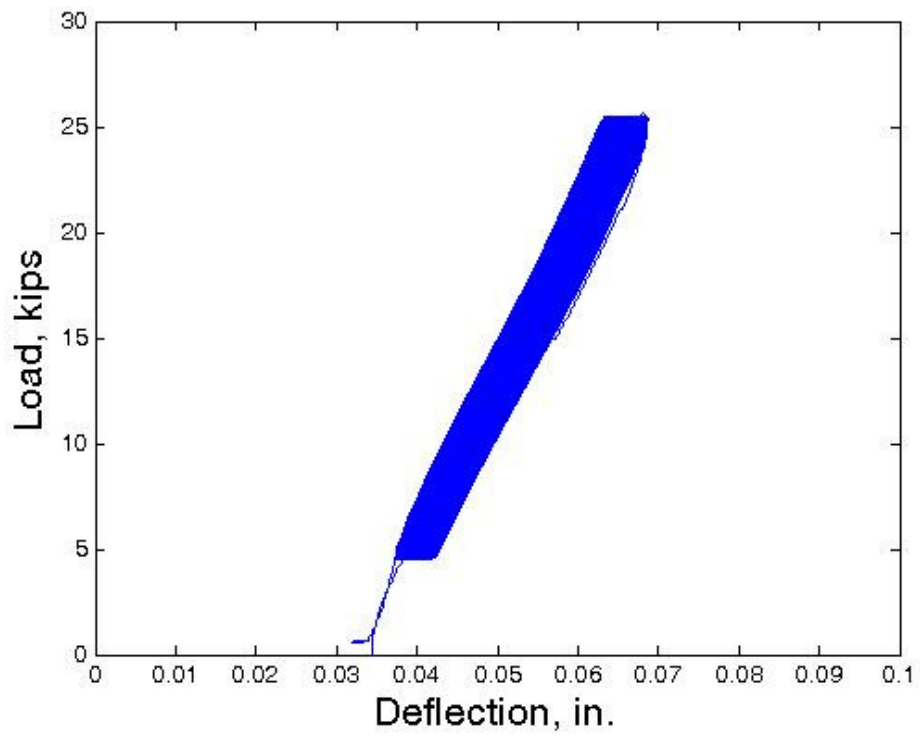


Figure A.7: F4 Load versus deflection

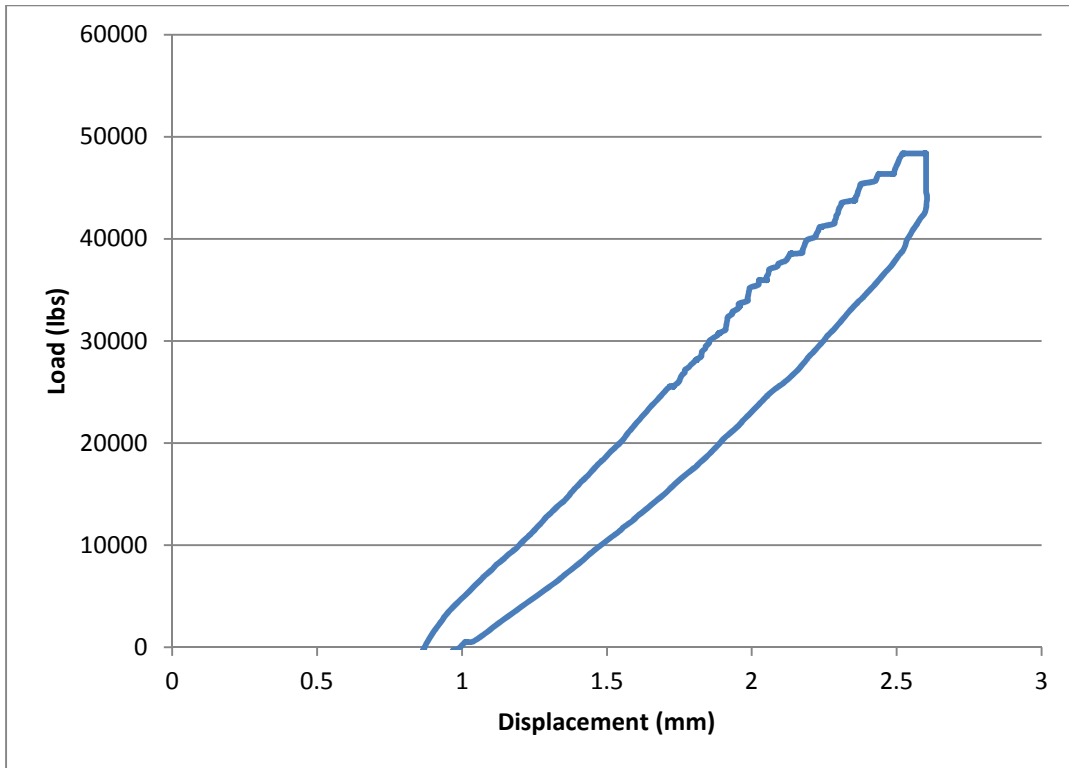


Figure A.8: Load vs. deflection for service level overload 2

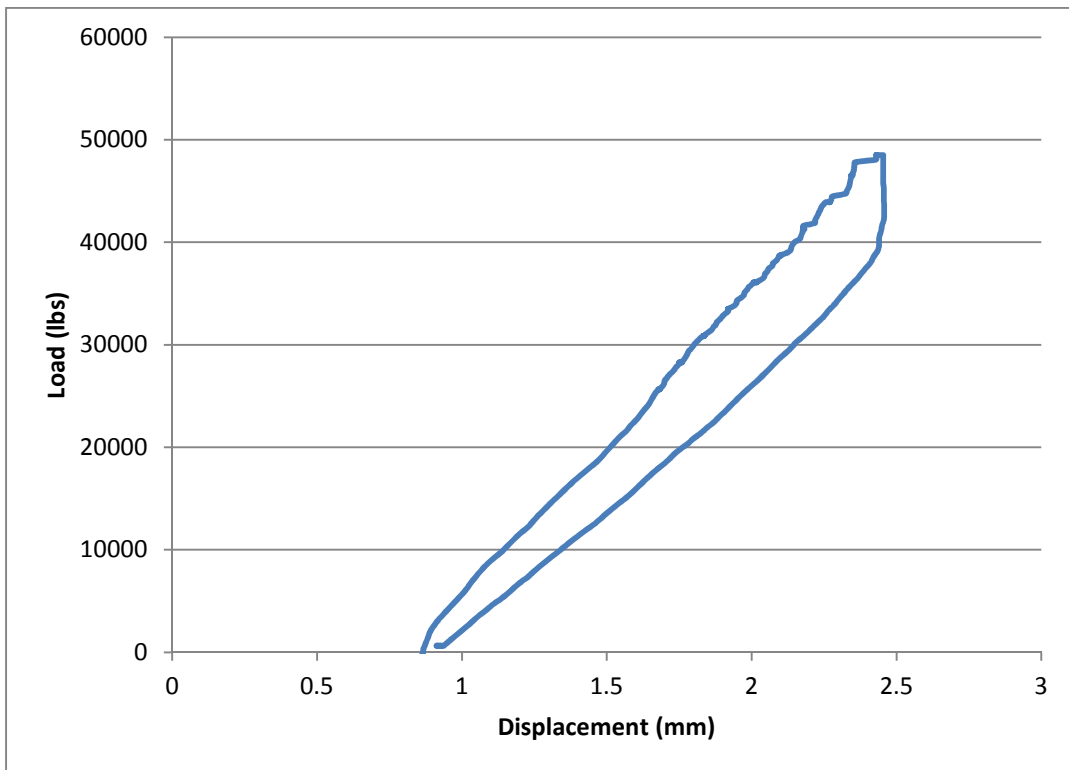


Figure A.9: Load vs. deflection for service level overload 3